A SCENARIO APPROACH FOR OPERATIONAL PLANNING WITH DEEP RENEWABLES IN POWER SYSTEMS

A Dissertation

by

MOHAMMAD SADEGH MODARRESI

Submitted to the Office of Graduate and Professional Studies of
Texas A&M University
in partial fulfillment of the requirements for the degree of

DOCTOR OF PHILOSOPHY

Chair of Committee,	Le Xie
Committee Members,	Chanan Singh
	Natarajan Gautam
	I-Hong Hou
Head of Department,	Miroslav M. Begovic

May 2019

Major Subject: Electrical and Computer Engineering

ABSTRACT

This work is both enabled by and motivated by the development of new resources and technologies into the power system market operation practice. On one hand, penetration level of uncertain generation resources is constantly increasing and on the other hand, retirement of some of the conventional energy resources like coal power plants makes market operations an attractive topic for both theoretical and state-of-the-art research. In addition, as generation uncertainty increases, it impacts the true cost of energy and causes it to be volatile and on average higher. This work targets flexibility enhancement to the grid to potentially eliminate the impact of uncertainty. Two different viewpoints in two different markets for electricity is targeted. This dissertation looks at the real-time market generation adequacy from the Independent System Operator's point of view, and the day-ahead scheduling of energy and reserve procurement from the market participant's point of view.

At the real time scale, the emphasis is on developing fast and reliable optimization techniques in solving look-ahead security constrained economic dispatch. The idea is when forecast accuracy gets sharper closer to the real-time and slower power plants retiring in recent years, market participants will spend more and more attention to the real-time market in comparison to the day ahead operation in terms of the energy market. To address it, a data-driven model with rigorous bounds on the risk is proposed. In particular, we formulate the Look-Ahead Security Constrained Economic Dispatch (LAED) problem using the scenario approach techniques. This approach takes historical sample data as input and guarantees a tunable probability of violating the constraints according to the input data size. Scalability of the approach to real power systems was tested on a 2000 bus synthetic grid. The performance of the solution was compared against state-of-the-art deterministic approach as well as a robust approach.

Although the real-time market is primarily for energy trading, the day-ahead market is the market for ancillary service trading. In this dissertation, at the day-ahead scale, the focus is on providing ancillary service to the grid by controlling the consumption of millions of privately owned

pool pumps in the US, while benefiting from energy arbitrage. A conceptual framework, a capacity assessment method, and an operational planning formulation to aggregate flexible loads such as in-ground swimming pool pumps for a reliable provision of spinning reserve is introduced. Enabled by the Internet of Things (IoT) technologies, many household loads offer tremendous opportunities for aggregated demand response at wholesale level markets. The spinning reserve market is one that fits well in the context of swimming pool pumps in many regions of the U.S. and around the world (e.g. Texas, California, Florida). This work offers rigorous treatment of the collective reliability of many pool pumps as firm generation capacity. Based on the reliability assessment, optimal scheduling of pool pumps is formulated and solved using the deterministic approach and the scenario approach. The case study is performed using empirical data from Electric Reliability Council of Texas (ERCOT). Cost-benefit analysis based on a city suggests the potential business viability of the proposed framework.

DEDICATION

To my family and the Oasis family

ACKNOWLEDGMENTS

I would like to thank my Ph.D. adviser and friend, Dr. Le Xie who supported me through all the hardships I faced during my life in the US. His strength to lead by example in academic and non-academic subjects made me a better researcher, leader, and personality through these years.

I also would like to thank Dr. Chanan Singh for his support and valuable inputs through our work on the swimming pool subject and my other two committee members Dr. Natarajan Gautam and Dr. I-Hong Hou.

I would like to thank Dr. Algo Carè, Dr. Marco Campi, Dr. Simone Garatti and Dr. Kumar for their theoretical support through our collaboration in the scenario based dispatch.

I'm also grateful to be a part of an amazing research group with the lead of Dr. Xie. I want to thank my dear office-mate, Xinbo Geng for all the bits of help. I would also like to thank current and former students of Dr. Xie: Dr. Anupam. A. Thatte, Tong Huang, Hao Ming, Rayan El Helou, Yuqi Zhou, Dr. Hung-Ming Chou, Dr. Omar A. Urquidez, Dr. Yingzhong(Gary) Gu, Dr. Dae-Hyun Choi, YuanYuan (Crystal) Li, Sean Chang, Jonathan M. Snodgrass, Dr. Bin Wang, Dr. Yang Bai, and Dr. Xiaowen Lai.

I would like to thank my friends who were beside me for part or all of this Ph.D.: Mohammad Reza Sanatkar, Bob and Suzanne Achgill, Mary & Elizabeth Krath, Rebecca & Pejman Honarmandi, Hongxiang "Caspeř" Fù, Tyler Scott, Dr. Daniel Humphrey, Zain Rizvi, Ehsan Kafai, and my longtime friend Amir Bahraei.

I would like to thanks ECE and ISS staff of Texas A&M for their support specially Tammy Carda, Anni Brunker, Lisa Cauvel, Wayne Matous, Enrique J. Terrazas, and Katie Bryan.

Above all, I would like to thank my family, my mom, and dad, my sisters, nieces and nephews, and brothers-in-law for their love and support.

CONTRIBUTORS AND FUNDING SOURCES

Contributors

This work was supported by a dissertation committee consisting of Professor Le Xie, Professor Chanan Singh, and Dr. I-Hong Hou of the Department of Electrical and Computer Engineering and Professor Natarajan Gautam of the Department of Industrial & Systems Engineering.

The computation in chapter 2 was performed with the help of Texas A&M High Performance Research Computing (HPRC) center.

Funding Sources

Graduate study was supported in part by NSF Contracts ECCS-1760554 and ECCS-1839616, and the Power Systems Engineering Research Center (PSERC).

NOMENCLATURE

Sets:

Δ	The uncertainty set.
$\Delta_{\mathcal{S}}$	Set of $\mathcal{S}$ scenarios which are randomly extracted from uncertainty set Δ, $\delta_s \in \Delta_{\mathcal{S}}$.
$\mathcal{A}$	Set of scenarios to be eliminated by any arbitrary rule.
c_{g_i}	Submitted energy offer curve of unit g_i.
G, G^r	Set of operating generators, set of renewable generation resources, $G^r \subset G$.
$\mathcal{X}$	Set of feasible solutions for the scenario problem (convex and closed), $x \in \mathcal{X}$.

Parameters and constants:

ϵ, ϵ_k	Risk parameter, risk parameter after discarding k scenarios.
$\overline{\epsilon}$	Upper bound of the risk parameter in the a-posteriori stage.
$\nu^{\star}_{\mathcal{S}}$	Number of support constraints.
β	Confidence parameter.
π^E, π^R	Energy and spinning reserve price forecast.
$\pi^E_{\delta_i}, \pi^R_{\delta_i}$	Energy and spinning reserve price forecast scenario.
$B_{\mathbf{g}}$	Nodal generation incident matrix.
$B_{\mathbf{l}}$	Nodal load incident matrix.
d	Number of decision variables in the scenario problem $\mathcal{X} \subset R^d$.
F, $\overline{F}$	Branches flow vector, branches capacity vector.
g_i, l_j	Symbols of generator g_i and load point l_j.
$\mathcal{H}_d^{req}$	Required number hours a pool pump needs to operate to keep the cleaned water standards.
$\mathcal{H}_d^{max}$	Maximum number hours a pool pump needs to operate to keep the cleaned water standards.

N_b, N_g N_l, N_k	Number of buses, generators, loads and lines.
$PTDF_{\mathbf{e}}$	Extended power transfer distribution factor matrix.
$p_{\mathbf{g}}$	Generation forecast error matrix, ($p_{g_i} = 0 \quad \forall g_i \notin G^r$).
$p_{\mathbf{l}}$	Load forecast error matrix.
$\mathcal{P}_{\mathbf{n}}$	Nodal power injection matrix.
$\hat{\mathcal{P}}_{\mathbf{l}}$	Load forecast matrix.
RU_{g_i}	Upward ramp rate capacity of unit g_i.
RD_{g_i}	Downward ramp rate capacity of unit g_i.
$SR^{req}[t]$	Market participant's Spinning reserve requirement for each time t.
T	Number of intervals of the LAED.
U^{max}	Maximum MW capacity from swimming pools equipped with required devices.
z	Objective function.
Decision variables	
$\mathcal{P}_{\mathbf{g}}$	Power generation matrix.
P_{g_i}	Power generation for g_i.
$u[t]$	Pools energy consumption schedule.
$sr^{DAM}[t]$	Spinning reserve to be purchased from the day-ahead market.

TABLE OF CONTENTS

Page

LIST OF FIGURES

FIGURE Page

LIST OF TABLES

TABLE Page

1. INTRODUCTION

1.1 Motivation

The increasing level of uncertain renewable energy resources in the power grid has been a driving force of research innovation in the past decade around the world. This, compounded by the retirement of many coal-fired fossil fuel generation sources, has introduced substantial challenges in the reliable and efficient operation of the electric grid. As an example, the Electric Reliability Council of Texas (ERCOT) has 23.4% of total generation capacity as wind power and reached the record of the wind share in the total energy production (50%) on March 23, 2017. ERCOT generation portfolio is shown in Fig. 1.1 [1].

Such a change in the generation portfolio leads to many changes in both physical and market operations. This thesis tries to provide two solutions to this problem. One for the real-time scheduling from the system operator's point of view, and one from the physical level and from a market participant's point of view.

Fig. 1.2 illustrates timings of decisions for a particular delivery time and sides active in the process of decision making. As shown, there is a window of uncertainty between the time we make the decision and the actual delivery time in the energy market. To manage the uncertainties at the operating stage, four classes of complementary approaches have been proposed focusing on different angels of the decision making process in power systems. The first approach is to utilize controllable conventional generating units to compensate the uncertainty. A great body of research has focused on this topic in the past quarter of a century [2,3]. The main advantage of this approach is that the energy/reserve procured from conventional power plants is firm capacity and there is *almost* no uncertainty about the capacity of these resources to replace intermittency/contingency in modern power systems. However, it is costly because a certain capacity of power plants need to be dedicated to providing the reserve for the system while it can be used for the energy market. Furthermore, since the location of the source of uncertainty and load might be different, deliver-

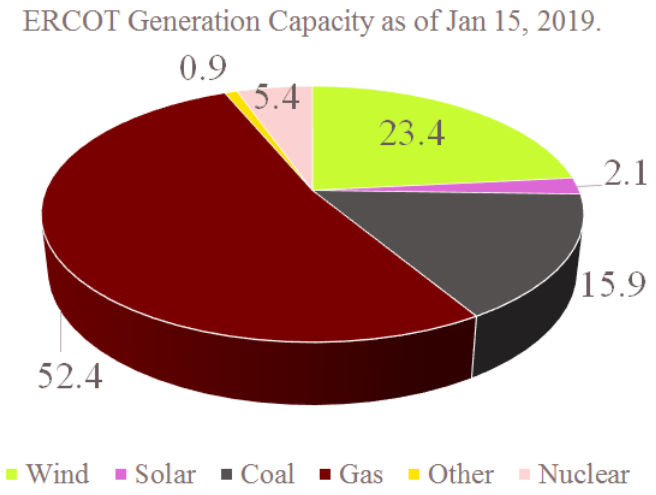

Figure 1.1: Generation mix in the ERCOT market.

ability of such reserve, when needed, is another challenge. Chapter 2 partly focuses a look-ahead real-time scheduling of these units to deal with growing uncertainty in the system.

The second option is holding some capacity of renewables and use it as reserve. With more mature power electronics and forecasting techniques, this option is in the transition from research into practice [4,5]. The third option is to install energy storage systems to manage uncertainty and enhance the reliability of power systems. Finding the optimal location and storage sizing is one of the major challenges in the third option since capital investment cost for these resources are still high [6, 7]. The fourth option is using the adaptability of load to provide flexibility to the bulk power system. This option is becoming more practical with the increasing availability of two-way communication through the Internet. Chapter 3 focuses on this option. In particular, we present a framework of aggregating many end-use loads, to provide reliable reserves with *little or no impact on consumer's comfort*.

1.2 Organization

This dissertation addresses one problem in two separate viewpoints using a data-driven technique. It consists of two parts each covering one of the two major power markets, two major market products, and two prospective. As shown in Fig. 1.3 in each of the two markets, a different

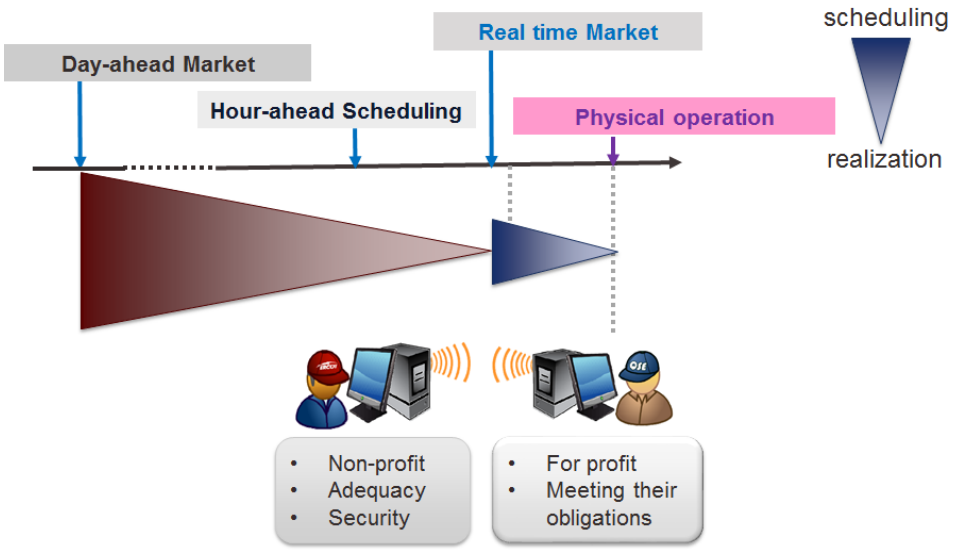

Figure 1.2: Decision making in power systems.

problem is being solved and the nature of uncertainty is different. While methods being proposed in this dissertation target different markets from different viewpoints, the endgame of them is the same: adding more flexibility to the system and enhance the reliability of power system while the cost of operation is not becoming overly conservative.

For the purpose of improving theoretical approaches in solving a fundamental power system scheduling problem, economic dispatch problem, we introduce a scenario based approach with tunable level of risk in Chapter 2, but we use its results in both Chapter 2 and Chapter 3. More precisely, Chapter 2 focuses on the real-time market, from the point of view of the Independent System Operator (ISO). The market product on the spotlight in this section is energy. The focus in this section is generation adequacy in the look-ahead intervals when having high uncertainty in the net load. Since the above-mentioned uncertainties are often not well defined in terms of an underlying probability distribution or range of uncertainty and by the recent advancements in a type of chance constrained programming named scenario approach, we formulate a scenario based look ahead dispatch in this section. This approach is shown to have rigorous bounds on the maximum probability of violating constraints in the a posteriori test, for a given historical sample from the uncertain resources [8]. The proposed approach has two stages.

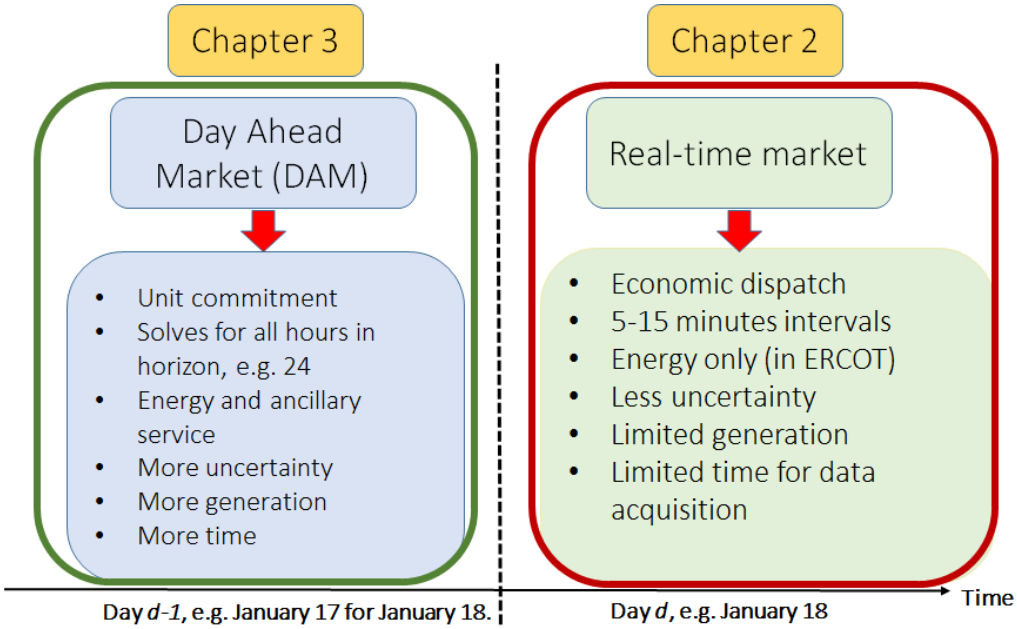

Figure 1.3: Two different markets: State of the art.

One is the a-priori stage where the decision is being made and the risk parameters are being defined before observing the results. In this stage, we showed that if transmission congestion is not an issue, e.g. midnight hours when abundant transmission capacity is available, the number of samples needed to guarantee a certain risk level does not grow with the size of the system. We also showed how *bad* samples can be discarded with a controlled impact on the risk threshold. This approach is called sampling and discarding which we trade risk for performance. It is particularly significant because it prevents overly conservative solutions that most of robust approached return by discarding such scenarios. We showed cost reduction while risk is below the threshold theory defines for a realistic 2000-bus test system on the footprint of Texas. It is showed that the proposed a-priori method can return results with a guaranteed performance with a cost much closer to the deterministic results than robust results.

The second stage is the a-posteriori stage. In this stage, we consider all constraints and we typically start the scenario problem using available samples. We solve the problem and by observing the *complexity* of the results, we define a-posteriori risk parameters. Complexity will be rigorously

defined in Chapter 2. Precisely we know the risk of our results after solving the problem. We showed that for the structure of economic dispatch, this risk can be much smaller than the risk a-priori theory provides.

In Chapter 3, we try to use capacity of the demand to gain flexibility for the system while preserving privacy and comfort of customers. The main focus in on the spinning reserve market at the day-ahead stage. The viewpoint is the market participant's following the requirements of the ISO. The idea is to aggregate the capacity of millions of available pool pumps and participate them in the spinning reserve market. A reliability assessment, operational planning, and cost-benefit analysis are be performed [9]. It is shown first how reliable capacity can be gained from unreliable resources, then it is shown how a trader or market participant can play in the market with this capacity using either forecast of the prices or scenarios for the prices for energy and spinning reserve market products.

1.3 Contributions

The dissertation has achieved the following contributions:

- Proposed a scalable scenario based economic dispatch with a tunable level of risk for the real-time, or close to real-time power systems operation,
- Exploited the structure of the state-of-the-art economic dispatch problem and dramatically reduced the size of the existing scenario based economic dispatch methods,
- Based upon the importance of transmission constraints at each particular hour, we proposed an a-priori (neglecting transmission constraints) and an a-posteriori (including transmission constraints) solution to such problem making the size of samples limited and the risk of the decision level below a controlled threshold,
- Scenario reduction technique was recommended in the a-priori stage to prevent a potential conservative sample from making the entire scenario method conservative.

- A frameworks for aggregation of demand resources and their participation into the spinning reserve market was introduced, formulated and tested by performing the following steps:
  - To gain reliable capacity through unreliable loads, a reliability assessment frameworks was designed and modeled the reliability of the system
  - Given the reliable capacity to participate into the market, an operational planning stage was formulated and showed how energy and reserve co-optimization should be performed to maximize the profit
  - It was shown that a scenario-based solution can be much more beneficial and risk-averse compared to a deterministic one
  - A cost-benefit analysis showed promising financial benefits of such approach on a sample sat of customers in Dallas-TX.

2. SCENARIO-BASED ECONOMIC DISPATCH WITH TUNABLE RISK LEVELS IN HIGH-RENEWABLE POWER SYSTEMS[1]

2.1 Introduction

Increasing levels of uncertain distributed generation resources are being integrated into electric power systems. These new resources of energy are distributed both in the supply and the demand side. Wind generation and utility-scale solar farms are two examples of these resources on the supply side, and roof-top solar PVs is an example of these resources on the demand side. For instance, wind power currently comprises 22% of total generation capacity in Electric Reliability Council of Texas (ERCOT) and the record of the wind share in the total energy production in any one hour reached 54% on October 27, 2017 [10]. ERCOT also plans to integrate 8.3-11.9% of solar generation and retire a substantial portion of its coal generation resources over the next decade [11]. Similar trends are also occurring elsewhere in the world. Operational planning such as unit commitment and dispatch will need to be revisited in order to reliably absorb these new resources at an affordable cost.

Due to the uncertainty and variability introduced by renewables, there has been a large body of literature devoted to solving Optimal Power Flow (OPF) [12, 13]. At the day-ahead stage, there has been a large body of literature applying stochastic [14, 15] and robust [16, 17] optimization techniques in unit commitment problems, which involve integer variables. At the near real-time stage, there have been similar efforts on improving the performance of economic dispatch, or the optimal power flow problems. Among these efforts is look-ahead economic dispatch (LAED), which employs a moving window optimization to account for inter-temporal variations in the near term [18–21]. The key idea is to extend the optimization horizon from one-time interval to multiple time-coupled intervals, allowing for early detection and better management of ramping/congestion related variations. However, how to model uncertainty for such a problem is still under exploration

[1]This section is in part a reprint of the material in the following paper: Reprinted with permission from M. Sadegh Modarresi, Le Xie, *et al.*, "Scenario-based Economic Dispatch with Tunable Risk Levels in High-renewable Power Systems," in IEEE Transactions on Power Systems. DOI: 10.1109/TPWRS.2018.2874464, Copyright 2018, IEEE.

[22–27].

One can categorize the methods dealing with uncertainty into two general approaches. The first class of methods, which are categorized as robust optimization [28–30] try to address *any* realization of uncertainty. However, robust optimization guarantees feasibility only if realizations of uncertainty occur inside the predefined uncertainty set or dynamically evolving uncertainty set, and, second, the extent of introduced conservativeness is generally unknown [31].

The second approach consists in finding a solution that satisfies the constraints with a predefined (usually high) probability —chance-constrained programming (CCP). CCP often offers a trade-off between the level of conservativeness of the results and feasibility of the problem. CCP is NP-hard in general. Methods to deal with CCP include: finding a deterministic equivalent to the chance-constrained program [32], Big-M approach [33, 34], robust counterpart [35, 36], and the scenario approach [37, 38].

With the proliferation of sensors and computational power, it is becoming increasingly desirable to obtain insights from empirical data and observations. Scenario approach as a sample-based optimization techniques has several features that makes it desirable for operational decision making: (1) it is driven purely by samples of empirical data; (2) it provides theoretical guarantees on the risk of violating the constraints; (3) it might be able to present a much tighter upper bound on the risk after observing complexity of the solution, and (4) it provides the option of dropping some realizations of uncertainty or relaxing the constraints while keeping violation probabilities within defined bounds.

The scenario approach deals with high levels of uncertain resources and provides quantifiable risk levels at the implementation stage. Much of the uncertainties arise from the high penetration of distributed energy resources (DERs). There have been a number of efforts to exploit the scenario approach theory in the general field of optimization, control [39, 40], and power system adequacy and security assessment [41–45]. This work is an effort to exploit the potential of the scenario approach theory for real-time scheduling and dispatch with high level of renewable resource penetration. In particular, the focus of the Chapter is on the scalability of the scenario theory to the

real-time power system operation which will be discussed in great details in Section 2.3.

The theoretical guarantees provided by the scenario approach can be *a-priori* (before collecting data) or *a-posteriori* (after computing a solution $x^\star$ based on the collected data). Correspondingly, depending on the chosen type of guarantee, the implementation of the scenario approach can be different.

Specifically, according to the a-priori results, it is possible to determine the number of scenarios that are required to attain a specified level of risk with high confidence. In this case, the scenario algorithm consists of the following steps: Step 1, specify the risk tolerance and the level of confidence in the results; Step 2, acquire an adequate dataset of a size that guarantees the risk and confidence levels; Step 3: Solve the problem (finding $x^\star$) taking only the sampled scenarios into account; and Step 4 (optional), eliminate a subset of scenarios from the sample set, using *any* rule, resulting in a new quantifiable risk parameter, but with a solution $x^{\star\prime}$ with lower cost, $z(x^{\star\prime}) \leq z(x^\star)$ (trading risk for performance).

Along the a-posteriori approach, instead, the scenario algorithm is run with a given dataset of any size. Then, after computing the solution, one can analyze its complexity (defined precisely in Section 2.3), and, by studying the risk jointly with the complexity, one can obtain a more clear knowledge of the actual risk of the scenario solution. This process is called *Wait-and-Judge approach* in [46]. It will be shown that this can play a key role vis-a-vis the scalability of the scenario approach method for bulk power systems applications.

The main contributions of this Chapter are as follows:

- A scenario approach-based formulation of LAED (Sc-LAED) that provides a guarantee on the risk level for any underlying distribution of uncertainty in the generation and/or demand is proposed.

- Conditions on the size of the dataset are derived under which the risk does not exceed a certain threshold with high probability.

- To address scalability of scenario approach theory to the real time power system operation, it

is shown that there are cases where the size of the dataset needed to guarantee a risk threshold is independent of the size of LAED (i.e. the number of generators). Moreover in general, it is shown that the risk guarantees can be tightened to a more precise upper bound a-posteriori by observing the complexity of the Sc-LAED solution.

- Scenario reduction in Sc-LAED is also considered: one can use any rule to eliminate scenarios and thereby avoid overly conservative solutions, with measurable risk parameter changes.

The rest of this Chapter is organized as follows. Section 2.2 presents the formulation of the LAED. Section 2.3 presents the methods and key theoretical results of the scenario-based dispatch. Section 2.4 presents case studies using a 2000-bus test case. Conclusions and future work are presented in Section 2.5.

2.2 Taxonomy of Look-ahead Economic Dispatch Under Uncertainty

A comparison between different LAED problem formulations is presented in this section. State of the art approaches in solving LAED are briefly discussed along with the proposed formulation for the Sc-LAED. The results in the first decision interval, *e.g.*, $t = 1$ are binding and the decisions for future intervals are considered as advisory and subject to change during future dispatch intervals.

2.2.1 Deterministic, stochastic and robust LAED

The most common approach to look-ahead economic dispatch is a deterministic one (2.1). The dispatch aims at balancing the deterministic forecasted demand with least cost while satisfying the constraints. This type of dispatch uses the least number of decision variables and/or constraints, and it is naturally formulated as a linear programming problem. Therefore it is easier to adopt in real-time market clearing processes. However, it was not designed to take decisions against forecast uncertainty:

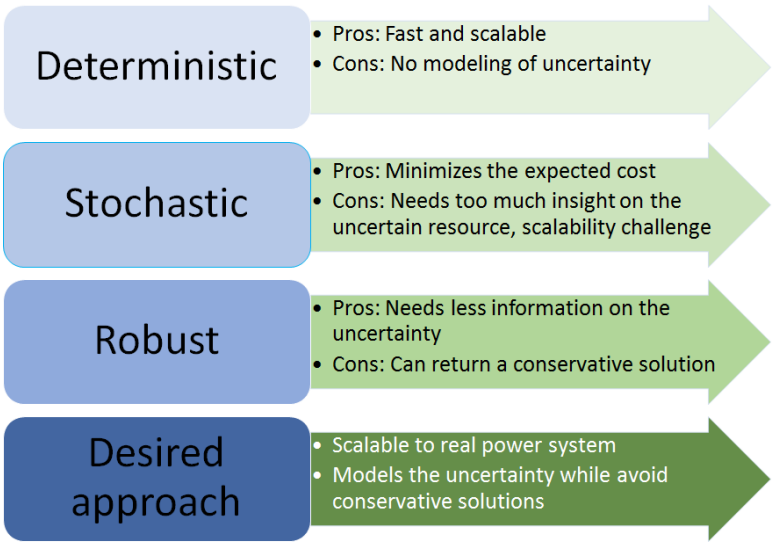

Figure 2.1: A comparison between weakness and strength of existing LAED approaches: The desired approach would avoid weaknesses while carrying the strength of existing approaches

$$\min_{P_{g_i}[t]} \quad z = \sum_{t=1}^{T} \sum_{i=1}^{N_g} c_{g_i}[t] P_{g_i}[t] \tag{2.1a}$$

$$\text{s.t.} \quad \sum_{i=1}^{N_g} P_{g_i}[t] = \sum_{j=1}^{N_l} \hat{P}_{l_j}[t] \quad \forall t = 1, 2, \dots T, \tag{2.1b}$$

$$-\overline{F} \leq F[t] \leq \overline{F}, \quad \forall t = 1, 2, \dots T, \tag{2.1c}$$

$$RD_{g_i} \leq P_{g_i}[t] - P_{g_i}[t-1] \leq RU_{g_i} \tag{2.1d}$$

$$\forall t = 1, 2, \dots T, \forall i,$$

$$P_{g_i}^{min}[t] \leq P_{g_i}[t] \leq P_{g_i}^{max}[t] \quad \forall t = 1, 2, \dots T, \forall i. \tag{2.1e}$$

Supply and demand balance is enforced by (2.1b). Inequalities (2.1c), (2.1d), and (2.1e) are transmission flow limits, generator ramp-up and ramp-down constraints, and offered minimum and maximum generator capacities respectively for each interval. Line flow limits are modeled as element-wise inequalities in (2.1c), where $F = PTDF_{\mathbf{e}} \times \mathcal{P}_{\mathbf{n}}$. $PTDF_{\mathbf{e}}$ is the extended power transfer distribution factor matrix with a zero column vector inserted on the slack bus. Therefore

the size of this matrix at each time t is $N_k \times N_b$ and $\mathcal{P}_{\mathbf{n}}$ is the nodal power injection matrix [47]. $\mathcal{P}_{\mathbf{n}}$ can be calculated as (2.2). The forecast errors for generation and load are not being considered in the deterministic formulation and will be discussed in Subsection 2.2.2. Elements of incident matrices, $B^{\mathbf{g}}$ and $B^{\mathbf{l}}$, for each node n are as (2.3) and (2.4).

$$\mathcal{P}_{\mathbf{n}} = B_{\mathbf{g}}(P_{\mathbf{g}} + p_{\mathbf{g}}) - B_{\mathbf{l}}(\hat{P}_{\mathbf{l}} + p_{\mathbf{l}}) \tag{2.2}$$

$$b^{\mathbf{g}}_{n,g_i} = \left\{ \begin{array}{ll} 1 & \text{if } g_i \xrightarrow[\text{bus}]{\text{connected to}} n \\ 0 & \text{otherwise} \end{array} \right\}, \tag{2.3}$$

$$b^{\mathbf{l}}_{n,l_j} = \left\{ \begin{array}{ll} 1 & \text{if } l_j \xrightarrow[\text{bus}]{\text{connected to}} n \\ 0 & \text{otherwise} \end{array} \right\}. \tag{2.4}$$

As mentioned, the deterministic LAED is scalable and fast. Furtheurmore, the solution of deterministic LAED is not conservative. For a market that requires a solution every 5-15 minutes, this is the most essential part to be met. Otherwise, the system operators will end of being reluctant performing it. However, there is no insight into the dependability of the solution. In other words, the system operators know that the solution given the forecasted level of wind/solar/load for future intervals exists, but with some errors in the forecasted values, there might not be a feasible solution in the future intervals.

In contrast to the deterministic approach, stochastic and robust LAED consider the uncertainty for the non-binding time intervals. However, they lack a few drawbacks making them hard to be adopted by the market operations.

Stochastic LAED [25] minimizes the overall expected cost of dispatch by incorporating the probability distribution of the forecast error. This distribution should accurately reflect the underlying uncertainty for the results to be valid. The drawbacks of this type of dispatch are: First It might be challenging to attain accurate information about the uncertainty distribution, and moreover, it gets even more challenging when the number of uncertain resources increases in the system.

Second, this dispatch method is computationally challenging for large scale systems. Therefore stochastic approaches face a difficult path to be scalable for future power system operations.

In robust LAED, an optimal solution is sought that is feasible for *all* of the realizations of uncertainty in the system. Therefore, if robust LAED finds a feasible solution, then the problem is indeed feasible provided that the uncertainty set considered in the model accurately reflects the underlying uncertainty. In contrast to the stochastic approach, robust LAED requires less information about the underlying uncertainty, but can return conservative results. The robust LAED formulation that we follow in this Chapter is based upon [26]. This conservative results makes can get more severe as the number of uncertain resources increases. Therefore this approach aslo faces scalability challanges in a differet way than stochastic approach.

A summary of the discussion above was shown in Fig. 2.1. Deterministic methods lack the modeling of uncertainty and, Stochastic, and Robust methods might face scalability challenges. The desired approach for this problem is an approach that has strong points of all these three approaches and suffers the least from their drawbacks. In other words, a scalable approach that does not require too detail information about the uncertainty while keeping the solution non-conservative. We think the answer to this problem is the *Scenario approach*.

2.2.2 Scenario approach LAED

Sc-LAED is defined as in (2.5), where $\mathcal{S}$ scenarios, $\delta_1, \ldots, \delta_{\mathcal{S}}$, are extracted from an uncertainty set Δ according to a probability distribution $\mathbb{P}$, and are simultaneously enforced [37, 48]. The main difference between the Sc-LAED formulation and robust LAED is in their approach toward uncertainty. While some robust LAED methods confine the borders of the uncertainty set (e.g., at $\mu \pm 3\sigma$), [26, 49], this choice impacts on the robustness and the conservatism of the results in a way that is difficult to quantify and deal with. On the other hand, the scenario approach is a direct approach, that is, data (the sampled scenarios) are used directly in (2.5), without any preliminary design of the uncertainty set. Thus, in Sc-LAED, the set of the uncertain values for which the constraints are enforced is the set of the sampled scenarios, and, as we shall see, there are theorems that show how the number of sampled scenarios can be used to tune the probability

that the obtained solution is satisfied by the unobserved uncertain values.

A crucial fact is that knowledge of the probability measure $\mathbb{P}$ over scenarios is not required: all that is required is a historical set of scenarios from the past that have already occurred. This sets the scenario approach apart from classic stochastic approaches where $\mathbb{P}$ is assumed to be known.

Note also that it is often the case that $\mathbb{P}$ is only implicitly defined by a complex model of the reality. In this case, valid scenarios (i.e., scenarios that are independent and identically distributed (i.i.d.)) can be generated by simulations, e.g. by resorting to statistical weather models [50]. The key theoretical guarantee provided by the scenario approach is that there is a rigorous upper bound on the level of risk associated with this type of dispatch, along with specified confidence level. For more discussion on the fundamental differences between the scenario approach and other approaches the reader is referred to [51].

$$\min_{P_{g_i}[t]} \quad z = \sum_{t=1}^{T} \sum_{i=1}^{N_g} c_{g_i}[t] P_{g_i}[t] \tag{2.5a}$$

$$\text{s.t.} \quad \sum_{i=1}^{N_g} P_{g_i}[t] = \sum_{j=1}^{N_l} \hat{P}_{l_j}[t], \quad t = 1, \tag{2.5b}$$

$$\sum_{i=1}^{N_g} P_{g_i}[t] \geq \sum_{j=1}^{N_l} \hat{P}_{l_j}[t] + p^{\delta_s}[t]$$

$$\forall \delta_s \in \Delta_{\mathcal{S}}, \forall t = 2, 3, \dots T, \tag{2.5c}$$

$$-\overline{F} \leq F^{\delta_s}[t] \leq \overline{F}, \quad \forall \delta_s \in \Delta_{\mathcal{S}}, \forall t = 1, 2, \dots T, \tag{2.5d}$$

$$RD_{g_i} \leq P_{g_i}[t] - P_{g_i}[t-1] \leq RU_{g_i}$$

$$\forall t = 1, 2, \dots T, \forall i, \tag{2.5e}$$

$$P_{g_i}^{min}[t] \leq P_{g_i}[t] \leq P_{g_i}^{max}[t] \quad \forall t = 1, 2, \dots T, \forall i. \tag{2.5f}$$

We now consider (2.5) in more details. The role of constraints are the same as that discussed for (2.1), with two differences. First the power balancing constraint is modeled as an equality constraint for the binding (and deterministic) interval, whereas it is modeled as an inequality for the non-binding (and subject to the uncertainty) interval. The intent of modeling (2.5c) as inequality

is to have enough capacity to respond to all unexpected changes in the load and generation [26]. Second, (2.5c) and (2.5d) are scenario-dependent constraints. $p^{\delta_s}[t]$ in (2.5c) is the net forecast error of the load and intermittent energy resources under scenario δ_s and is defined as: $p^{\delta_s}[t] = \sum_{j=1}^{N_l} p_{l_j}^{\delta_s}[t] - \sum_{i=1}^{N_g} p_{g_i}^{\delta_s}[t], \quad p_{g_i} = 0 \quad \forall g_i \notin G^r$. For resources with time-varying upper bound on generation, such as wind and solar, $P_{g_i}^{max}[t]$ is the maximum sustained limit of generation submitted by the resource at time t.

For simplicity, we rewrite (2.5) as (2.6), where (2.6b) represents (2.5b, 2.5e, 2.5f) and (2.6c) represents (2.5c, 2.5d):

$$\min_{x \in \mathcal{X}} \quad z = c^T x \tag{2.6a}$$

$$\text{s.t.} \quad f_1(x) \leq 0, \tag{2.6b}$$

$$f_2(x, \delta_s) \leq 0, \quad \forall \delta_s \in \Delta_{\mathcal{S}}. \tag{2.6c}$$

As we shall see, the number $\mathcal{S}$ of scenarios that guarantees a certain risk level can be computed *independently* of the underlying probability distribution of uncertainties, and mainly depends on the level of risk that one is willing to tolerate and the number of decision variables. If some scenarios cause unacceptable increments in cost (or result in infeasibility vis-a-vis dispatch), they can be removed from $\Delta_{\mathcal{S}}$ with controlled and quantifiable increase on the risk parameter, ϵ. Also, after finding a solution to (2.5), it can be shown that one can have access to the upper bound on conservativeness of the resulting solution. Further details on exploiting the scenario approach theory for the purpose of solving (2.5) are discussed in Section 2.3.

Before a deeper investigation of the scenario theory, a brief discussion about the impact of Sc-LAED on electricity market nodal pricing might be desirable. Locational Marginal Pricing is the main approach to define electricity prices and transmission congestion costs in many wholesale markets. To calculate the Locational Marginal Prices (LMPs) in Sc-LAED, a process similar to ex-post LMP calculation known as the *pricing run* in Independent System Operators (ISO) such as PJM, ISO New England, and NYISO [52] should occur. The inputs to the LMP calculation are

the results from the Sc-LAED binding interval and the subset of active transmission constraints. Essentially the results for $t = 1$ from (2.5) are used to find LMPs by solving a single interval problem. There are different approaches to calculate the *ex-post* LMPs such as [52–54]. The Appendix describes one of the most common approaches based on [55, 56] for the structure of our problem as (2.5).

Sc-LAED does not have a direct impact on markets clearing before the real-time market. For instance, Financial Transmission Rights (FTRs) allow market participants to hedge against transmission congestion charges present in the day-ahead market [57]. However, Sc-LAED might have an impact on market participants profiting from the differences between real-time and day-ahead prices. For instance, for the case of virtual transactions. The value of these products depends on the differences between day-ahead and real-time prices. Without a detailed simulation study, it is difficult to comment on the impact of Sc-LAED compared to conventional dispatch in terms of impact on Virtual trading profit/loss.

2.2.3 Scenario vs Robust LAED

The scenario approach and the robust approach differ at a very conceptual level and comparing them requires a clear assessment of the underlying modeling assumptions. The statement that, as the number of scenarios tends to infinity, the scenario solution tends to the robust solution is true (modulo details) only if we assume that the uncertain set in the robust problem coincides with the support of the probability distribution of the scenarios. While this can be expected at a conceptual level, this is typically not true in practice, where the robust decision-maker vacillates between two opposite options: on the one hand, the need to be robust suggests to design an all-encompassing uncertainty set; on the other hand, the need to have a feasible solution, or at least a good objective value, suggests to design an uncertainty set that is smaller than the set of all the uncertain values that are possible in principle.

When uncertain values are generated according to a known probability distribution, one can design the uncertain set in such a way that it will contain an uncertain value with high probability, say probability p. This is the case in our numerical set-up, where scenarios have a Gaussian

distribution but the uncertain set in the robust approach is bounded and is obtained by neglecting the tails of the Gaussian distribution. However, there are many degrees of freedom in shaping the uncertain set. Polyhedral uncertain sets are often computationally handy, but it is a fact that in general one could achieve better objective values by shaping the uncertain set in other ways (which are computationally more challenging). As a result, it is almost always the case that the robust solution that is built based on a p-probability uncertain set will satisfy a constraint with probability far larger than p. As we shall explain at the end of this comment, this is also what happens in our numerical example.

Summing up, it is fair to say that the robust approach is an indirect method: first, one designs the uncertain set, and then a solution is computed based on such uncertain set. The scenario approach, instead, takes a direct approach: one skips the explicit design of the uncertain set and computes a solution based directly on the sampled scenarios. In doing so, the set of the uncertain values for which the constraints are satisfied is implicitly shaped by the sampled scenarios, and theorems show how to tune its probability by choosing the number of sampled scenarios. It is also remarkable that, in order to apply the scenario approach, the probability distribution according to which scenarios are sampled is not required to be known, and typically it is not. We just need a sufficient number of sampled scenarios.

The sampled scenarios must be independent and identically distributed (i.i.d.): they must be sampled independently from the same (possibly unknown) probability distribution that describes the uncertainty, and based on which the violation probability of the solution is defined. As a matter of fact, sampling methods that do not preserve the i.i.d. property are not valid in our set-up.

2.3 Computational Algorithm to Solve the Scenario Approach Economic Dispatch

The Sc-LAED approach prescribes to solve a convex optimization problem whose constraints depend on sampled scenarios, which are expected to carry knowledge about the future behavior of load, wind and solar resources. Precisely, a set of scenarios $\Delta_S \subset \Delta$ is obtained by sampling the uncertainty set Δ, and the problem (2.6) is then solved for the scenarios belonging to Δ_S. Problem (2.6) is an instance of what in the literature is called a Scenario Problem (or Scenario Program, see

e.g., [37, 38, 46]), and we will denote it by $SP_{\mathcal{S}}$.

The central question that arises is therefore the following: how much one can rely on $\Delta_{\mathcal{S}}$ as a representative of the whole uncertainty set Δ, which includes all the possible (yet unseen) realizations of the stochastic uncertainty? In order to address this question in quantitative terms, we have to define rigorously the risk of the solution $x^\star_{\mathcal{S}}$, as the probability that this solution will turn out to be infeasible for another realization of the stochastic uncertainty. This concept is made precise by defining the violation probability of $x^\star_{\mathcal{S}}$ as follows.

Definition 1 (Violation probability (or risk) of $x^\star_{\mathcal{S}}$)**.** *Let $x^\star_{\mathcal{S}} \in \mathcal{X}_{\mathcal{S}}$ be the solution to $SP_{\mathcal{S}}$. Then the violation probability (or risk) of $x^\star_{\mathcal{S}}$ is denoted by $V(x^\star_{\mathcal{S}})$ and defined as*

$$V(x^\star_{\mathcal{S}}) := \mathbb{P}\{\delta \in \Delta : f_2(x^\star, \delta) > 0\}, \tag{2.7}$$

where we recall that $\mathbb{P}$ is the probability distribution over Δ according to which the scenarios are sampled in an independent and identically distributed way.

Clearly, the risk depends on the set of extracted scenarios, and therefore it has a stochastic variability. Nevertheless, in [37] it was proven that there are conditions under which the risk is distributed according to a beta distribution, irrespective of the distribution of the sampling probability $\mathbb{P}$. More in general, the results in [37], and in following contributions, allow one to compute upper-bounds to the risk that hold true with high confidence. A crucial role in the theory of the scenario approach is played by the concept of support constraint, which is defined as follows.

Definition 2 (Support Constraint)**.** *The scenario-dependent constraint corresponding to sample δ_s, $s \in \{1, 2, ..., \mathcal{S}\}$, is a support constraint for $SP_{\mathcal{S}}$, if its removal improves the solution of $SP_{\mathcal{S}}$, i.e., if it decreases the optimal cost (2.6a).*

We are now ready to state the main results of the theory of the scenario approach and exploit them in the present context. Subsections 2.3.1 and 2.3.2 focus on the a-priori evaluation of the risk, where we use samples from the uncertainty set to guarantee a certain level of risk with high confidence. Based on the results in these two subsections and the analysis of the Sc-LAED problem

in the absence of congestion, we propose a data-driven procedure that we call Algorithm 1. In Subsection 2.3.3, we consider the case when there is congestion and show that, in spite of the high number of scenarios that are required by the a-priori approach, it is still possible to make useful and accurate claims on the risk after observing the complexity of the obtained solution (a-posteriori evaluation). Conclusions are drawn and a data-driven procedure that exploits a-posteriori evaluation is proposed (Algorithm 2).

2.3.1 The a-priori scenario approach method

The main theorem in [37] is the following one.

Theorem 1. *With the assumption that (2.6) returns a unique solution, it holds that*

$$\mathbb{P}^{\mathcal{S}}\{V(x^\star_{\mathcal{S}}) > \epsilon\} \leq \sum_{i=0}^{d-1} \binom{\mathcal{S}}{i} \epsilon^i (1-\epsilon)^{\mathcal{S}-i}, \tag{2.8}$$

where $\mathbb{P}^{\mathcal{S}}$ is the probability distribution taken over $\delta_1, \ldots, \delta_{\mathcal{S}}$, which is a product probability due to independence.

The right-hand side of (2.8) is the tail of a beta distribution with parameters (d, $\mathcal{S} - d + 1$). As $\mathcal{S}$ grows, the tail goes exponentially to zero [37]. Fixing a small β, say $\beta = 10^{-6}$, one can easily find the smallest number of samples $\mathcal{S}$ such that $\sum_{i=0}^{d-1} \binom{\mathcal{S}}{i} \epsilon^i (1-\epsilon)^{\mathcal{S}-i} < \beta$ holds true, so that the right-hand side of (2.8) is less than the specified β. Then, one can claim that with high confidence $1-\beta$ the risk $V(x^\star_{\mathcal{S}})$ of the scenario solution with $\mathcal{S}$ scenarios is no larger than ϵ. Note that the right-hand side of (2.8) does not depend on $\mathbb{P}$. This is remarkable and shows that, in order to guarantee that $V(x^\star_{\mathcal{S}}) \leq \epsilon$ with confidence $1-\beta$, we do not need to know $\mathbb{P}$.

A graphical representation of the roles of the risk parameter ϵ and the confidence parameter β is shown in Fig. 2.2. The cube on the left is $\Delta_{\mathcal{S}}$, the set of all the possible $\mathcal{S}$-tuples of scenarios. A point in this cube can be identified with an instance of $\Delta_{\mathcal{S}}$, i.e., with a particular set of scenarios $\{\delta_1, \delta_2, \ldots, \delta_{\mathcal{S}}\}$ that is obtained by randomly sampling $\mathcal{S}$ scenarios from Δ according to the probability distribution $\mathbb{P}$. For this sample $\Delta_{\mathcal{S}}$, there is a set of feasible solutions χ which does not violate any of the constraints for any of the scenarios in $\Delta_{\mathcal{S}}$. This is depicted in the middle of Fig.

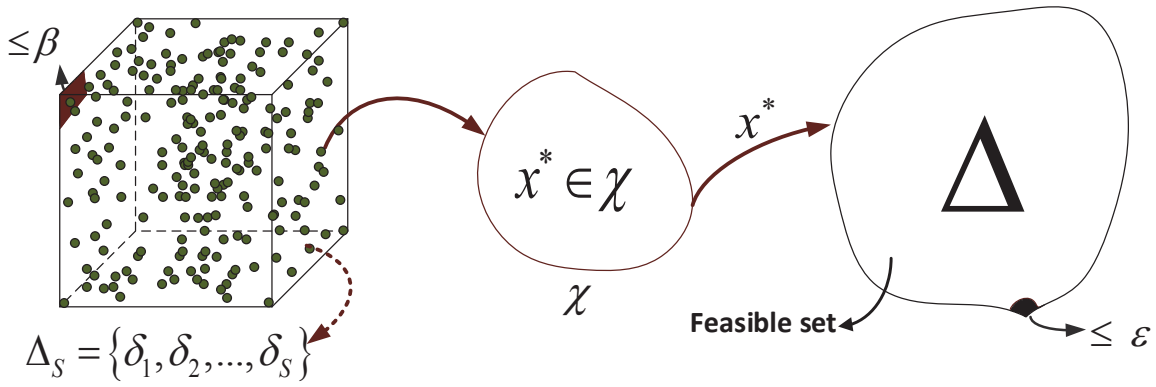

Figure 2.2: Illustration of the scenario approach.

2.2. An optimal solution $x^\star_{\mathcal{S}}$ is then determined for this set $\Delta_{\mathcal{S}}$ of scenarios. The set of scenarios δ belonging to Δ for which $f_2(x^\star_{\mathcal{S}}, \delta) > 0$ (i.e. the constraint in (2.6) is violated) is called the violation region and it is the region shaded black in the right in Fig. 2.2. This region has probability $V(x^\star_{\mathcal{S}})$. We would like this probability to be always smaller than the risk parameter ϵ. However, $V(x^\star_{\mathcal{S}})$ has a variability as it depends on the sampled scenarios $\Delta_{\mathcal{S}}$ through $x^\star_{\mathcal{S}}$, and it will happen that $V(x^\star_{\mathcal{S}}) > \epsilon$ for certain samples $\Delta_{\mathcal{S}}$ that are in a *bad set*. Such bad set is depicted as the black region in the cube on the left. Theorem 1 guarantees that, if the right-hand side of (2.8) is smaller than $\beta \in (0, 1)$, the bad set has a probability that is smaller than β (with respect to the product measure $\mathbb{P}^{\mathcal{S}}$).

An explicit formula to find $\mathcal{S}$, which returns a slightly more conservative number of samples, is given below in (2.9), which is taken from [58]. As can be seen, the number of samples needed grows linearly with the dimension the optimization being performed and $\frac{1}{\epsilon}$, but it is not as sensitive to β.

Lemma 1. *Under the same conditions as Theorem 1, if*

$$\mathcal{S} \geq \frac{2}{\epsilon}(ln\frac{1}{\beta} + d) \tag{2.9}$$

then $\mathbb{P}^{\mathcal{S}}\{V(x^\star_{\mathcal{S}}) > \epsilon\} \leq \beta$.

We now consider the structure of the Sc-LAED problem more explicitly. It is remarkable that in (2.5), only (2.5c) and (2.5d) consist of scenario dependent constraints defined by the net-load forecast error at each bus. Eliminating (2.5d) (for now), one can observe that at most $T-1$ constraints can be active and indeed be support constraints. This is due to the fact that for each $t = 2, \ldots, T$, the constraints in (2.5c) are half-spaces with the same slope but different displacement, so that no more than one can be active at the same time. Therefore, the number of support constraints for (2.5) is no more than $T-1$ with probability one. In view of this fact, the same formula in (2.8) can be applied by replacing d with $T-1$, see e.g. [59, 60]. This prevents the number of samples from growing to very large numbers when congestion is not in the picture. The reduction in the number of required samples in this special case helps the scalability of the problem and shows that the number of samples can be independent of the number of generators and the number of buses in the system, and it only depends on the number of look-ahead intervals $T-1$, ϵ and β.

For a general case, and for bulk power systems application, satisfying (2.8) or (2.9) will require a large number of samples. This is an instance of a well known issue in the literature on the scenario approach, and several solutions are available that range from multiple steps or iterative procedures, see [61] and references therein, to regularization schemes, [62]. Among them, the recently proposed "wait and judge approach", [46], is of particular interest in the case of Sc-LAED, because it allows one to compute the upper bound on the risk of the solution as a function of the complexity of the obtained solution. In this way, useful upper bounds can be obtained also when a small amount of scenarios is available. This approach will be discussed in 2.3.3.

It is also important to remark that, in general, among the sampled scenarios, there might be some extreme scenarios that can lead to excessively conservative results in terms of cost function. In the following subsection 2.3.2, we show how to eliminate such scenarios while taking under control the increase in the risk bounds.

2.3.2 Sampling and Discarding Approach in Sc-LAED

The Sampling and Discarding Approach [38] is one technique in the scenario approach theory to trade risk for performance. Essentially the cost of Sc-LAED is reduced by eliminating scenarios

of choice, but the price paid is an increase in the guaranteed risk. Let $\mathcal{A}$ be the discarded scenarios among those in $\Delta_{\mathcal{S}}$, and let $|\mathcal{A}|$ be the cardinality of $\mathcal{A}$. If the following relation is satisfied,

$$\binom{|\mathcal{A}|+d-1}{|\mathcal{A}|}\sum_{i=0}^{|\mathcal{A}|+d-1}\binom{\mathcal{S}}{i}\epsilon^i(1-\epsilon)^{\mathcal{S}-i}\leq\beta, \tag{2.10}$$

then the solution $x^{\star}_{\mathcal{S}-|\mathcal{A}|}$ that is obtained by removing the scenarios in $\mathcal{A}$ from $\Delta_{\mathcal{S}}$ has a risk no larger than ϵ, with high confidence $1-\beta$.

Usually, the support constraints with highest improvement in the cost of Sc-LAED are removed sequentially, by selecting the scenarios with the highest Lagrange multipliers. However, any other elimination rule is valid. For the stated result to hold true, the number of scenarios to be discarded ($|\mathcal{A}|$) should be defined a-priori, while choosing $|\mathcal{A}|$ a-posteriori is possible at the price of a (usually minor) degradation in the overall confidence (typically, the confidence becomes $1-K\beta$ instead of $1-\beta$, where K is the total number of values of $|\mathcal{A}|$ that one is willing to accept; for a detailed discussion on this point, see the discussion before equation (4) in [38]).

Combining the results of Theorem 1 and (2.10), a procedure (Algorithm 1) is here proposed for the case when no congestion is expected. The user inputs a desired risk parameter ϵ_0. As explained above, exploring alternative solutions through scenario removal comes at the cost of degrading the guaranteed risk. Hence, the user also sets a modified risk parameter, $\tilde{\epsilon}\geq\epsilon_0$, which is still acceptable for practical purposes and that should be preferred to ϵ_0 only if the gain in terms of cost function is significant. Similarly, a desired confidence parameter β_0 is specified together with a degraded confidence parameter $\tilde{\beta}\geq\beta_0$ that is still acceptable for practical purposes. These parameters together determine how many scenarios can be safely removed before a solution is returned by the algorithm, that is, they allow the system operator to trade risk for performance in a safe way.

Algorithm 1 for Sc-LAED in the absence of congestion

1. **INPUT:** ϵ_0**,** $\tilde{\epsilon}$**,** β_0**,** $\tilde{\beta}$**,** T

2. Compute $\mathcal{S}$ that satisfies (2.9) when ϵ,β,d in (2.9) are replaced by $\epsilon_0,\beta_0,T-1$ respectively.

3. **for** $i = 1, 2, \ldots$

   (a) Find a valid ϵ_i that satisfies inequality (2.10) where d and $|\mathcal{A}|$ in (2.10) are replaced by $T - 1$ and i respectively.

   (b) **if** ($\epsilon_i > \tilde{\epsilon}$ **or** $(i+1)\beta > \tilde{\beta}$), **then go to** step 4.

4. Sample $\mathcal{S}$ scenarios and compute $x^\star_\mathcal{S}$ by solving (2.6).

5. **if** ($c^T x^\star_\mathcal{S}$ is satisfactory or $i = 1$) **then OUTPUT:** $x^\star_\mathcal{S}$, its guaranteed risk ϵ_0 and the confidence $(1 - i\beta_0)$; **else**

6. **for** $k = 1, \ldots, i-1$

   (a) Remove the worst k scenarios from $\delta_1, \ldots, \delta_\mathcal{S}$ in (2.6) and compute the solution $x^\star_{\mathcal{S}-k}$ with $\mathcal{S} - k$ scenarios.

   (b) If ($c^T x^\star_{\mathcal{S}-k}$ is satisfactory **or** k is equal to $i - 1$), **then OUTPUT:** $x^\star_{\mathcal{S}-k}$, its guaranteed risk ϵ_k and the confidence $(1 - i\beta_0)$.

2.3.3 The a-posteriori scenario approach method

Convex optimization in dimension d has, at most, d support constraints [48, 63]. For the class of *fully supported problems* (when a problem in dimension d has exactly d support constraints with probability one), strict equality holds instead of inequality in (2.8). However, in many engineering applications, the problem being solved is not a fully supported problem. For instance, as discussed in Sc-LAED, when the system is not congested the number of support constraints is always far less than the number of decision variables. In this subsection, we study $V(x_\mathcal{S})$ jointly with the complexity of the solution, defined below as $\nu^\star_\mathcal{S}$ for the general case where transmission constraints are considered.

Definition 3 (Complexity)**.** *$\nu^\star_\mathcal{S}$, the complexity of the solution $x^*_\mathcal{S}$ to $SP_\mathcal{S}$, is the number of the support constraints for $SP_\mathcal{S}$.*

Complexity in Sc-LAED consists of the (at most $T-1$) support constraints corresponding to the generation adequacy constraint in (2.5c) plus *possibly* some support constraints for (2.5d), which cannot be predicted before solving (2.5).

The relation between risk and complexity was first studied in [46]. The results of [46] provide an upper bound on the risk after computing the solution. See Theorem 2 below.

Theorem 2. *For program (2.6) with $\mathcal{S} > d$, for any $\tau = 0, 1, 2, ..., d$, the polynomial (2.11) below, with t as variable has one and only one solution in $(0, 1)$.*

$$\frac{\beta}{\mathcal{S}+1}\sum_{i=\tau}^{\mathcal{S}}\binom{i}{\tau}t^{i-\tau} - \binom{\mathcal{S}}{\tau}t^{\mathcal{S}-\tau} = 0. \tag{2.11}$$

We denote this solution by $t(\tau)$. Defining $\overline{\epsilon}(\tau) = 1 - t(\tau)$ under the assumption of non-degeneracy and uniqueness of the solution [46], it holds that

$$\mathbb{P}^{\mathcal{S}}\{V(x^\star_{\mathcal{S}}) \leq \overline{\epsilon}(\nu^\star_{\mathcal{S}})\} \geq 1 - \beta. \tag{2.12}$$

The results after observing $\nu^\star_{\mathcal{S}}$ support constraints, compared to the original bound from [37] for the Synthetic Texas System [64] with $T = 2$ in (2.5), are showed in Fig. 2.3. When $\nu^\star_{\mathcal{S}} \ll d$, the results improve significantly. This allows one to make significant claims on the risk even when the number of sampled scenarios is relatively small. For example, for the setting described in Fig. 2.3, an upper bound of $\epsilon = 0.5967$ is obtained by using Theorem 1 with $\mathcal{S} = 2000$. On the other hand, with the same number of scenarios, observing $\nu^\star_{\mathcal{S}} = 18$ allows one to claim $\overline{\epsilon}(\nu^\star_{\mathcal{S}}) = 0.0262$ as an upper bound thanks to Theorem 2.

The following Algorithm 2 exploits Theorem 2 to compute upper bounds on the risk of the scenario solution when congestion is expected, so that d cannot be replaced by $T-1$ in Theorem 1, and the number of scenarios $\mathcal{S}$ cannot be increased to the values required by Theorem 1. In this algorithm $\mathcal{S}$ is supposed to be given and typically it accounts for existing computational/data collection limitations.

Algorithm 2 for Sc-LAED when congestion is expected

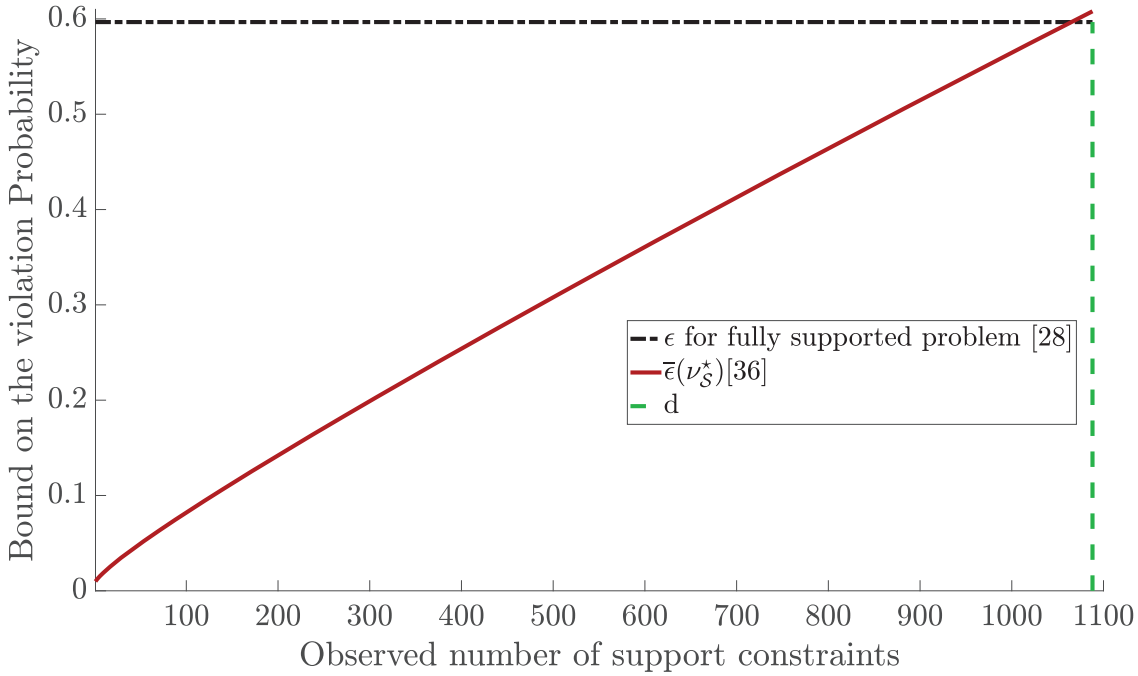

Figure 2.3: Upper bound on the risk for $\mathcal{S} = 2000$, $d = 1088$. The vertical axis denotes values of $V(x^\star_{\mathcal{S}})$, and horizontal axis denotes values of $\nu^\star_{\mathcal{S}}$. The distance between the black dotted line and the red curve is the improvement on the risk bounds provided by Theorem. 2.

1. **INPUT:** $\mathcal{S}$**,** β

2. Compute $\bar{\epsilon}(\tau)$, $\tau = 0, \ldots, d$ according to Theorem 2.

3. Sample $\mathcal{S}$ scenarios and solve (2.6); obtain $x^\star_{\mathcal{S}}$ and count the number of support constraints $\nu^\star_{\mathcal{S}}$.

4. **OUTPUT:** $x^\star_{\mathcal{S}}$ and the upper bound on the risk $\bar{\epsilon}(\nu^\star_{\mathcal{S}})$.

In conclusion, Algorithm 1 is the choice when the system operator does not expect congestion in the next T intervals. On the other hand, when congestion is in the picture, the a-posteriori approach (Algorithm 2) should be employed.

Considering that, in real life, the LAED problem is solved several times along a time horizon, one can try to guess $\nu^\star_{\mathcal{S}}$ for a new instance of Sc-LAED based on the past solutions, so as to adjust $\mathcal{S}$ accordingly. For example, $\nu^\star_{\mathcal{S}}[t-1]$, *i.e.*, the number of support constraints at the previous time

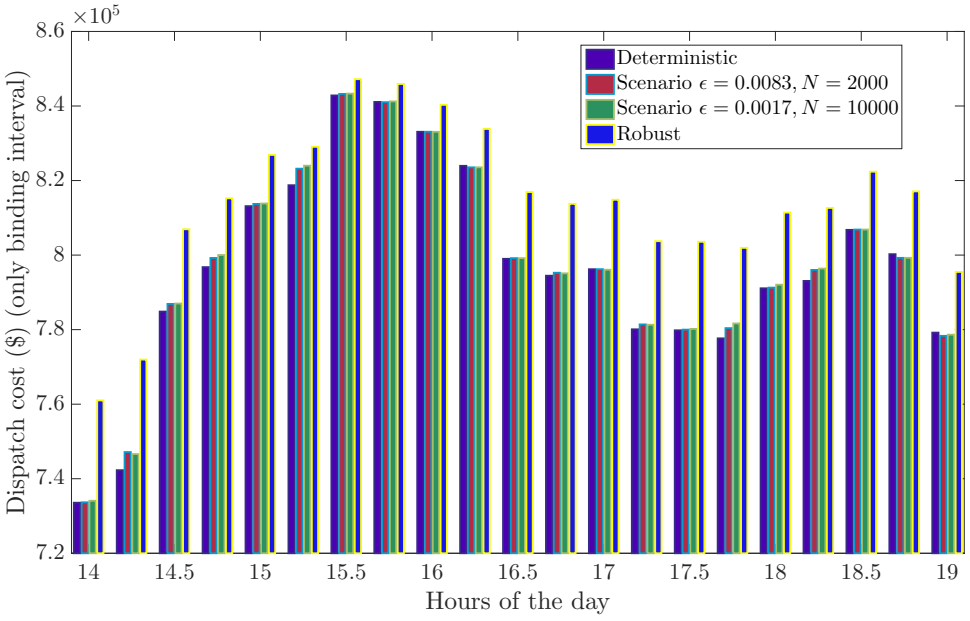

Figure 2.4: Comparison of the Dispatch Cost during the peak hours of the day using different methods.

step, can be used as a starting estimate for the number of support constraints at time t. When $\nu^\star_{\mathcal{S}}[t-1] \ll \nu^\star_{\mathcal{S}}[t]$ and $\mathcal{S}$ samples are not sufficient to guarantee the desired risk level, one might sample new scenarios according to an iterative algorithm. Iterative schemes in this line of thought are the subject of ongoing research.

2.4 Case Study

In this section, we test the proposed approach on a 2000-bus synthetic grid on a footprint of Texas [64]. This system consists of 544 generation units, with a portfolio of 367 gas, 39 coal, 4 nuclear, 25 hydro, 87 wind and 22 utility scale solar power plants. Nodes with wind/solar resources are where uncertainty exists. This can be generalized to DER aggregation and participation into the wholesale electricity market. 432 of these units are active during the study period (default setting in [64]). Its transmission network consist of 3206 transmission lines. Installed wind capacity is about 13% of the peak load, and installed solar capacity is less than 1% of the net load. MATPOWER [65] is used to obtain PTDF of the synthetic grid and confirm the accuracy of the base case modelings.

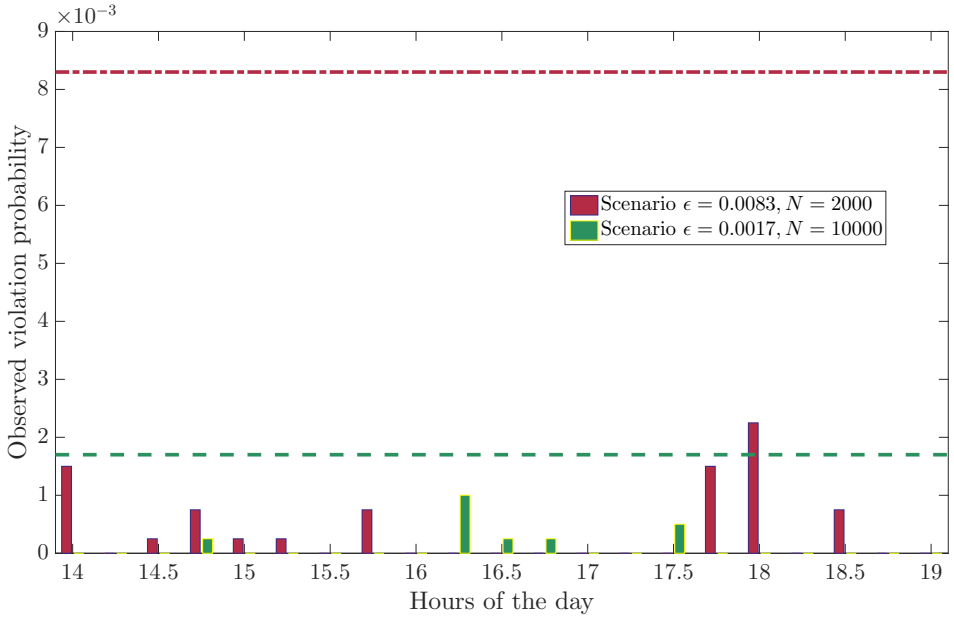

Figure 2.5: $V(x^{\star}_{\mathcal{S}})$ for two different scenario settings.

Where data was not given (such as the ramping capabilities of the units), the modifications were performed according to [19, 49]. In addition load and wind profiles were adapted from these references.

The optimization is performed for a 24 hour period (96 intervals). T in (2.5) is two, meaning that there is one deterministic and binding, and one uncertain, non-binding interval. For efficient illustration, in each of the following subsections, the focus will be on some different windows of the 96 intervals during a day. It is assumed that generators bid linearly into the real-time market. The uncertainty on each uncertain resource is distributed according to Gaussian distribution with mean μ equal to the nominal forecast and with standard deviation σ defined as the normalized standard deviation of the wind/solar forecast. A scenario is obtained by sampling the uncertainty instances from these distributions in an independent fashion. Information on the scenario generation mechanism was provided here for the sake of comparison only, and it must be remarked that the adopted method does not require that the underlying probability distribution be known. Deviations from forecasted values enter the net load scenarios as negative load. The confidence

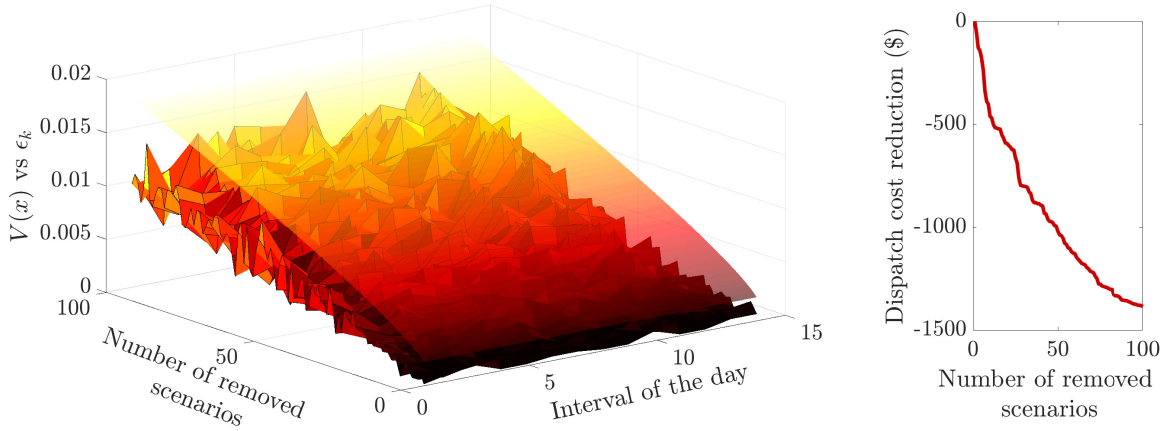

Figure 2.6: Sampling and discarding results: trading risk for performance. Left: Violation probability (Monte Carlo estimate with 10000 samples) located below ϵ_k. Right: Binding interval cost reduction in one interval after elimination of k scenarios.

parameter $\beta = 10^{-6}$ is used throughout the case study. The decision of each dispatch method is tested using 10000 *independent* scenarios extracted from the same uncertainty set.

This case study is divided into two parts. The focus of the first part is on the ramping events due to renewable integration in the system, illustrating the algorithm suggested in Subsections 2.3.1 and 2.3.2 with $d = 1$ in the absence of congestion in the system. The second part extends the original scenario theory to the results shown in Subsection 2.3.3 in the presence of line constraints. It is shown that by using the results in (2.12) it is possible to start with a sample size with almost no guarantee on the results and reach a very high confidence in the results by analyzing the complexity of the solution.

2.4.1 Extreme ramping test: Scenario vs deterministic and robust LAED

To simulate how different methods respond to the possibility of an extreme ramping event, we increased the wind/solar penetration threefold while increasing the load in the system by 18%. σ for each uncertain resource is 0.07μ, where we recall that μ is the forecast of wind and solar resources. A full Gaussian distribution is used to generate the scenarios for the scenario approach. Following the robust methodology in [26], we truncated the Gaussian distribution at $\mu \pm 3\sigma$ for the robust method.

The simulation is performed for two different sizes of scenarios, and compared to the deterministic and robust methods. The scenario sizes are 2000 and 10000, which correspond to $\epsilon = 0.0083$ and 0.0017 respectively using (2.8). As discussed in Section 2.2, the decision for the first interval is binding and the future interval is advisory. Therefore in Fig. 2.4, we compare the dispatch cost of the binding interval (where there is no uncertainty) using different approaches. We show peak hours in Fig. 2.4 because the system is more vulnerable to ramping events during these hours. As can be seen, the robust method has a clear offset in terms of the binding dispatch cost while the deterministic method carries the least cost of dispatch. However, the increment in the dispatch cost using the scenario method is small compared to the robust method. It should be noted that the generated sets of 2000 and 10000 scenarios are generated independently. Therefore there can be a few cases where the dispatch cost is higher with 2000 scenarios than with 10000.

Violation probabilities in the scenario approach are as expected and shown in Fig. 2.5. The robust method maintained the zero violation probability, while scenario LAED allowed some violations, but kept this violation below the corresponding ϵ. The $V(x^\star_{\mathcal{S}})$ for the deterministic LAED is 0.5029 for the hours shown in Fig. 2.5. Therefore, the scenario method successfully confines $V(x^\star_{\mathcal{S}}) \leq \epsilon$ with a cost much smaller than the robust method.

As forecast error is explicitly stated in the Sc-LAED problem by (p_{g_i}, $i = 1, \ldots, N_g$) and the load forecast errors (p_{l_j}, $j = 1, \ldots, N_l$): a scenario is the assignment of these $N_g + N_l$ values for each time $t = 2, \ldots, T$. For example, constraint (2.5c) is determined by the net forecast error, which at every time step is a linear combination of the $Ng + Nl$ uncertain quantities. The crucial fact here is that the interplay of the uncertainties coming from different sources is naturally taken into account by the scenario approach. In fact, in our numerical example, stochastic errors of different signs tend to cancel out in the net forecast error: the result is that the net forecast error is not so spread around zero, that is, it is not so different from the nominal case. On the other hand, this interplay is neglected in the robust approach, where the uncertain set in the robust approach is built by constructing a 3σ interval for each of the 109 uncertain wind and solar resources. A simple computation shows that there is a 25% probability that a new scenario that is sampled according

to the full (non-truncated) Gaussian distribution will not belong to the 3-sigma-based uncertain set that is used to solve the robust problem. Nonetheless, the robust solution turns out to violate a new constraint with a probability far smaller than 25%, a probability that is indistinguishable from 0% in our experiments. This is due to the fact that the construction of the uncertain set does not take into account how the uncertainty impacts on the actual constraints, i.e., the averaging effect due to the combinations of different sources of uncertainty is not exploited in the robust formulation.

Some extreme scenarios that can lead to conservative results might be included when samples are being collected randomly. We used 10000 scenarios in the previous section and dropped up to 100 of them. As mentioned in Section 2.3.2, the discarding strategy can be using any arbitrary rule. In this case, we discard the constraints whose removal maximizes the reduction of dispatch cost. As shown in Fig. 2.6 (right), when scenarios are being dropped, the performance, which in this case is the cost of the binding interval, is being improved. The performance improvement is traded for risk. Fig. 2.6 (left) shows $V(x^{\star}_{\mathcal{S}-k})$ and ϵ_k after dropping $k \in [1, 100]$ scenarios. The values of ϵ_k extracted from (2.10) are the values of the transparent plane depicted above the observed violation probabilities.

Trading risk for performance can be particularly helpful if dropping the first few scenarios significantly reduces the costs, as in the case of the first few scenarios in Fig. 2.6 (right).

2.4.2 Risk and complexity: Considering all constraints in the Sc-LAED

In this subsection, both network and ramping constraints are considered. Therefore it is no longer possible to know the exact number of support constraints prior to solving the problem. To be able to use the original line constraints in [64], we do not change wind and solar penetration in this section. However, to cause congestion, we changed the load by 5% at all nodes. The argument is that by making a guess that the number of support constraints is low, we can start with a very large ϵ, solve the problem, and by observing the results update our knowledge of ϵ. In this case we solved the problem with 870 scenarios, which is slightly more than the number of decision variables (which is 864). This leads to $\epsilon = 0.9996$. This means that $V(x^{\star}_{\mathcal{S}})$ can vary from 0 to 0.9996, so that Theorem 1 provides almost no information about $V(x^{\star}_{\mathcal{S}})$. However, an a-posteriori

upper bound for $V(x^\star_{\mathcal{S}})$ can be found by Theorem. 2.

For instance, when 3 constraints of support are observed in Sc-LAED, meaning that their removal changes the solution, the claim "$0 \leq V(x^\star_{\mathcal{S}}) \leq 0.0282$" can be delivered.

For the test case, a-posteriori results for the first 50 intervals of a day are summarized in Fig. 2.7. As can be seen, the observed number of support constraints (blue $\square$) is small, although congestion exists. The number of support constraints for this study varies between one, two and, for some intervals three, which is much smaller than $d = 864$ (while the a-priori results in [37] are for a fully supported problem, *i.e.*, $\nu^\star_{\mathcal{S}} = 864$ with probability one). Using Theorem 2, one can rigorously define an upper bound on the risk of dispatch for these intervals. Our knowledge about the upper level of $V(x)$ gets much sharper as shown by the black stars in Fig. 2.7 (compare $V(x) \leq 0.9996$ with the results). 10000 samples for each interval were used to estimate the violation probability: the resulting estimates are all within the theoretical bounds and are represented by the red $\diamondsuit$ in Fig. 2.7.

2.4.3 Discussion on the results

One question that might come to the authors will be, why the number of support constraints are low? We tested different congested systems and we concluded that the number of support scenarios are limited for an $N-1$ secured system. In other words, when the system is operable in today's standards and not at the verge of collapse, the number of support constraints are limited. However, as of today, we could not come with a proof for it.

To describe it more clearly, consider a system that some lines are congested. The question is: Does removing a scenario *improves* the objective function? Potentially by relieving the congestion that exists in the system? Based on our observation in many cases it does not, because other scenarios next to it still keep that constraint active.

For instance, consider a very simple system in Fig. 2.8 and assume the Pg1, Pg2 has unlimited ramping. The system is $N-1$ secured but congested. With $T = 2$ and forecasted wind=200 MW for the deterministic interval, t=1. In such a system the Pw[1,2]=150, Pg1[1,2]=150, Pg3[1,2]=0 and the objective function cost of economic dispatch is $150 \times 30 \times 2 = \$9000$. As can be seen,

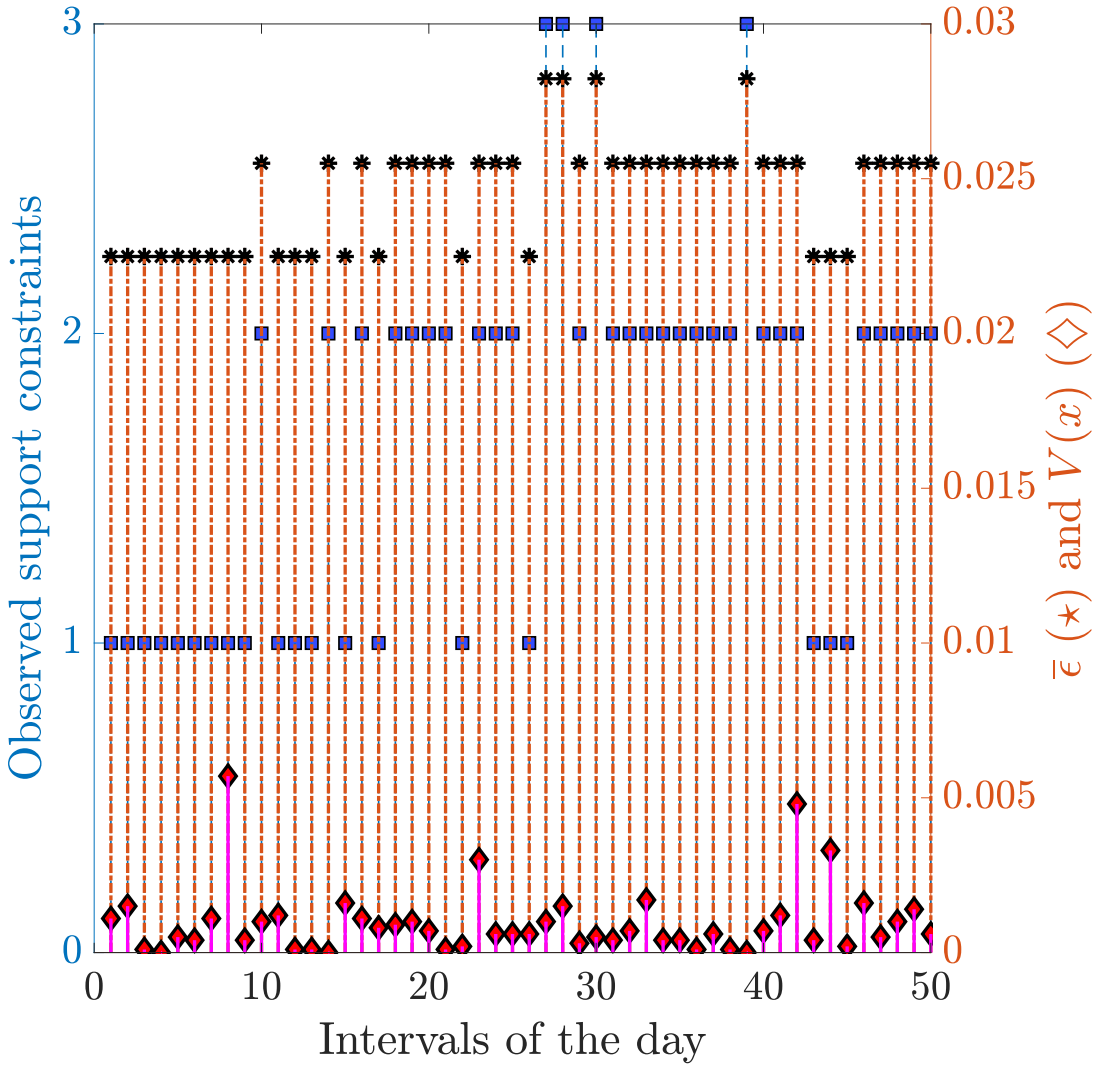

Figure 2.7: $\square$: Number of observed support constraints, $\diamondsuit$: violation probability (Monte Carlo estimate with 10000 samples) and $\star$, the upper bound on the violation probability based upon the complexity.

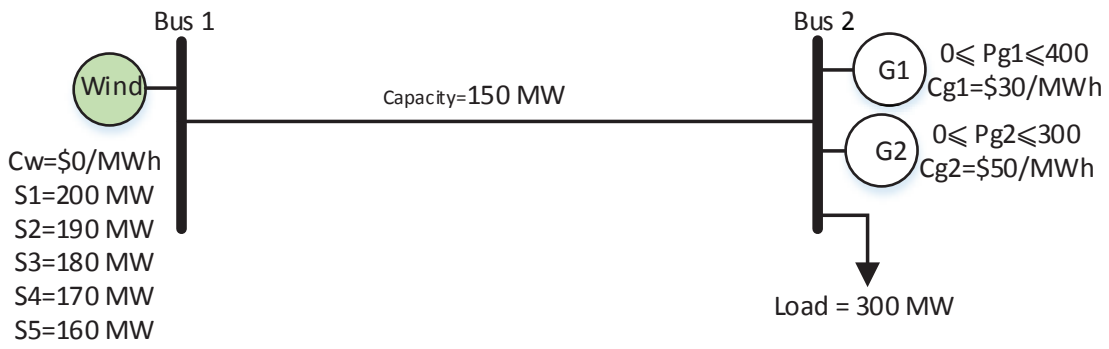

Figure 2.8: A simple example on support scenarios.

removing any of the scenarios do not improve the solution although the system is fully congested.

The example we showed was very simplistic to be able to illustrate this point: The level of congestion does not necessarily have an impact on the number of support constraints. However, our method is getting more powerful as the size of system increses.

It should also be noted that the average number of support scenarios depends on the number of scenarios being collected itself as well. For instance, if one extracts a bigger number of samples, the possibility of extracting a conservative sample will be higher and removing it might improve the solution. However, the beauty of the theory is that it the variations on the upper bound of violation probability in (11) and (12) will be different as well as shown in Fig. 2.9. As an example, observing two support constraint when we have $\mathcal{S} = 2000$ samples delivers (almost) the same level of a-posteriori risk parameter as observing 20 support constraints when $\mathcal{S} = 6000$. Therefore since we do not have a proof at the moment and as discussed in the conclusion, a good potential future work will be closing the loop between the number of support scenarios and number of collected scenarios in Sc-LAED.

The real-world application of scenario theory has been our main focus in this dissertation so we tried our best to make realistic assumptions both on parameters design and scalability of proposed strategy. To use Sc-LAED in everyday operation, two possibilities can be seen for the Sc-LAED. One is considering it as an adequacy assessment tool for reliability purposes. The tunable risk

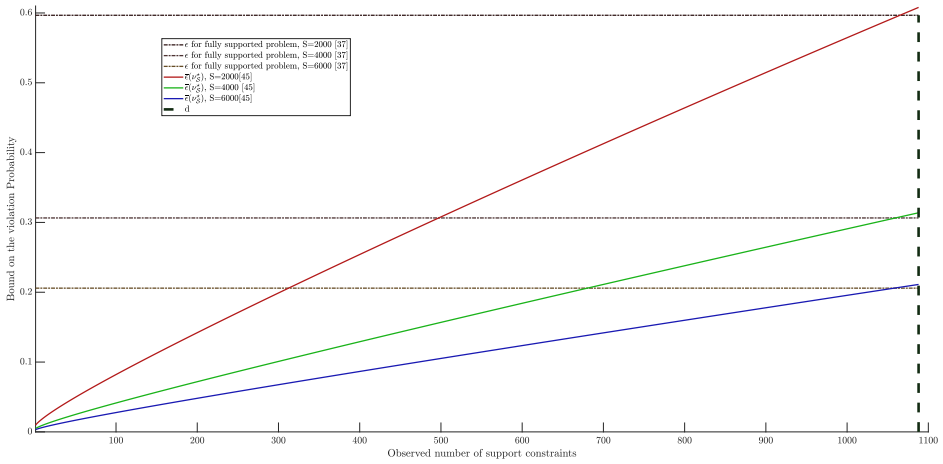

Figure 2.9: Different sample sizes and its impact on the a-priori and a-posteriori risk parameters, $\epsilon, \overline{\epsilon}$.

parameter Sc-LAED provides, as well as a-posteriori makes Sc-LAED attractive for this purpose. Since the operator uses Sc-LAED as an *advisory* tool, real-time prices won't get affected. However, the system overhead cost might increase if a further action is required, *i.e.* after seeing a high-risk level. Sc-LAED can also be used in the real-time market. As we addressed the editor's question, we discussed how different market products might be affected. Most importantly, the process of LMP formation can be similar to the ex-post LMP process currently being practiced in many ISOs using the results for the binding interval.

2.5 Conclusion

In this Chapter, the scenario approach for solving uncertain economic dispatch is introduced. It is shown that this approach does not require any knowledge of the underlying uncertainty distribution, yet yields a quantifiable level of risk in real-time economic dispatch. It is shown how the risk can be evaluated according to a-priori and a-posteriori mathematical results. Scalability of the problem is considered in both the a-priori and a-posteriori stages.

In the a-priori stage, it is shown that disregarding congestion, the number of samples needed does not increase with the size of the system. This fact bears several benefits: first, it makes

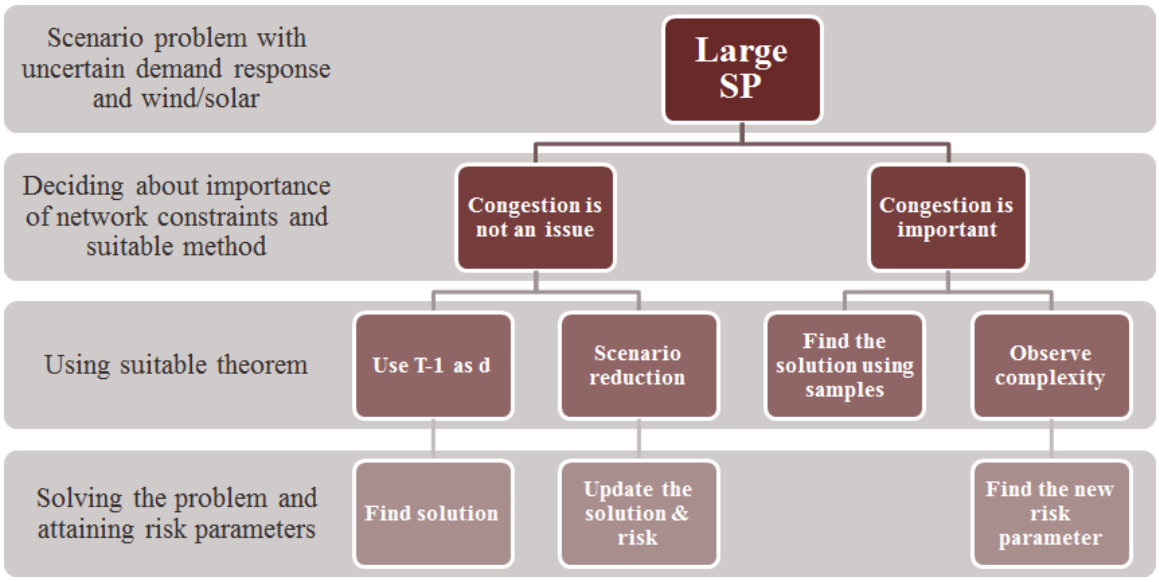

Figure 2.10: A graphical representation for selecting suitable Sc-LAED.

the process of collecting *i.i.d.* samples practical; second, it avoids both an overly conservative solution as well as high computational burden. Moreover, pessimistic scenarios can be neglected with controllable degradation of the violation probability.

In the a-posteriori stage, the risk of constraint violation can turn out to be much smaller than general a-priori, promising future scalability of the Sc-LAED for a congested case. The case study on a realistic power system suggests that scenario based LAED could provide a reliable solution with quantifiable bound on the conservativeness of the results. A summary of the above mentioned conclusion is shown in Fig. 2.10.

There is a need for more rigorous investigations of the correlation between the number of constraints of support and design parameters in Sc-LAED. Therefore, our future work will be mainly focused on the a-posteriori stage, where a procedure to start from a few scenarios and progressively aim towards desired $\bar{\epsilon}$ based on the observed number of support constraints, will be developed.

Practically speaking, the scenario approach strikes a good trade-off between deterministic and robust optimization-based dispatch. The ISO could potentially adopt scenario approach as a natural

step to manage uncertain DERs while keeping a tunable risk level at the ex-post stage. It could have direct benefits to both real-time and intra-day decision making process.

2.6 Acknowledgement

Portions of this research were conducted with the advanced computing resources provided by Texas A&M High Performance Research Computing.

3. DAY-AHEAD FLEXIBILITY PROCUREMENT FROM FLEXIBLE DEMAND[1]

3.1 Introduction

In this chapter, we focus on gaining flexibility from demand. In particular, we will be focused on aggregation swimming pools pumps to participate them in the energy market. We will focus on energy arbitrage as well as reserve procurement strategy given the resources. Two reliability assessment approaches along with two optimization approaches is described. One considers a simple approach and the other considers a more complex and complicated approach to reserve procurement and reliability assessment.

To gain flexibility from demand resources, there have been many efforts controlling smart appliance inside the houses to provide ancillary service to the grid. These range from appliances that are being used in everyday life such as refrigerators [66], to weather-dependent appliances like heating, ventilation, and air conditioning (HVAC) systems [67–69].

The above-mentioned works mainly focus on gaining benefits from the thermal inertia of refrigerators and HVAC systems. While controlling appliances inside the house for regulation reserve sounds logical (due to zero mean nature of this signal), these resources may not be ideally suitable to provide the spinning reserve to the grid. Spinning reserve deployment signal is not a zero mean signal and if deployed, the duration of its deployment can take from a few minutes to up to two hours [70, 71]. Due to the reliance of these resources on thermal inertia, they are unable to keep providing the spinning reserve for an extended period of time. In [70] the spinning reserve was only activated for a duration of 5-20 minutes for customers in California. Activation is through a *begin-curtailment* signal sent to customers. Customers remain curtailed until they receive an *end-curtailment* signal or their timer operates. Although no complaint from customers is registered in [70], it might not be true in all climate conditions. A study performed in [72] shows that indoor temperature can rise 4 degrees Fahrenheit in 5 minutes. Therefore, even if the spinning reserve is

[1]This section is in part a reprint of the material in the following papers: Reprinted with permission from M. Sadegh Modarresi, Le Xie, Chanan Singh, "Reserves from Controllable Swimming Pool Pumps: Reliability Assessment and Operational Planning," in Hawaii International Conference on System Sciences (HICSS), Copyright 2018, HICSS.

deployed for 20 minutes, the household temperature may become noticeably different at the end of the deployment of spinning reserve. It was shown in [70] that with less reliable generators (95% individual availability), load resources (with 90% individual availability) can be a more reliable resource than conventional power plants. Although the message for the given set of availability of power plants and loads is true, the reliability assessment is oversimplified. Since conventional power plants are highly maintained generation resources, their availability will remain constant during their lifetime. However, the reliability of one-way radio communication to a switch can decrease rapidly as time passes. If two-way radio communication is implemented, a discussion on maintaining the reliability is needed as well.

Meyn *et al.*, pioneered the usage of swimming pool pumps as an ancillary service provider [73–75]. The design of their work is to provide zero-mean regulation {up,down} reserve to the grid through randomized {ON,OFF} actuation of pool pumps in real-time. The control strategy is randomized and completely decentralized through mean field limit. The regulation signal is sent every 4 to 5 seconds and each pool pumps takes a sample of this signal every 30 minutes and arranges its behavior based on the number of hours it has been {ON,OFF} in a stochastic manner. When the number of pools is large enough (one million in the case of Florida), this randomized control provides firm regulation to the grid.

While the work of [73–75] addresses the issue of controlling loads to provide continuous AGC services, using the swimming pool pumps in the spinning reserve market might be a better fit for the ancillary service market due to inherent mechanisms of swimming pool pumps. At the beginning of the pumping cycle, pool pumps need a process of sending air out before pumping and circulation of the water begins. During this process, the electricity consumption of the single speed pump is well below the nominal level, *e.g.* 1.5 kW average (since it only sends air out) [76]. This process is called priming the pump. The priming process can take between 30 seconds to 30 minutes, with an average of 11 minutes [77]. Therefore system keeps regulation signal active for more than enough time because it does not receive enough response. By the time first-tier pumps finish priming, way more than enough pools received the regulation signal. Therefore an imbalance rebound happens.

However, since spinning reserve providers only need to reduce their consumption upon activation, priming will not have an impact on the quality of the reserve being gained from the pool pumps.

In this Chapter, we investigate the benefits of controlling swimming pool pumps {ON,OFF} status for providing *spinning reserve* to the wholesale level grid. We show that with proper investment and scheduling, these entities can provide the required level of reserve to the independent system operator (ISO). We show how the capacity of pools can be mapped to the exact quality and quantity from conventional power plants. We also formulate the day-ahead market (DAM) participation strategy as an aggregator. Furthermore, a data-driven procurement strategy is proposed. This approach is shown to reduce the realization cost of the aggregator in purchasing energy and reserve from the DAM. A cost-benefit analysis will also be demonstrated.

The key innovation in this part of the dissertation is suggested as follows:

- a firm reserve capacity is achieved through aggregation of many pool pumps in a rigorous reliability assessment framework.
- an optimal operational planning strategy for aggregators to provide spinning reserve is formulated.
- theoretical performance guarantee is provided for the scenario based operational planning technique.
- the performance guarantee will be shown to only depend on the size of the empirical data being used.

The rest of this Chapter is organized as follows: Section 3.2 provides a short background on spinning reserve market, and its procurement structure. Section 3.3 discusses the way it is possible to design a dominant strategy that benefits customers, aggregators, and the ISO. Section 3.4 introduces the reliability framework of finding the capacity of pool pumps to participate in the market along with a mode detailed reliability framework. Section 3.5 formulates and solves the operational planning problem from aggregators point of view using a deterministic and a chance-constrained

method. Section 3.6 provides a numerical example of the method introduced. Concluding remarks and future improvements needed for this work are described in Section 3.7.

3.2 Background on Spinning Reserves

Three major categories of ancillary service market products exist in most deregulated electricity markets: Regulation {up,down} reserve, spinning reserve, and non-spinning reserve. Regulation is generally a zero mean signal and providers should be able to respond to this signal within a few seconds. If the disturbance persists, the spinning reserve will replace regulation reserve, within 10 minutes of the first security constrained economic dispatch (SCED) after an event. Non-spinning reserve and (in some markets) supplemental reserve will be deployed if needed as well.

Prices of these products vary based on the system condition and structure of the day ahead market in these systems. The average price of these products in ERCOT from 2016-present is shown in Fig. 3.1. As can be seen, the spinning reserve is among the highest priced ancillary service product. While the prices always fluctuate across time and regions, this example suggests the potential of tapping into the spinning reserve markets via low-cost and reliable control of end-user loads.

Generation adequacy and security in a deregulated electricity market are achieved through communicating with market participants. Market participants are required to provide a share of spinning reserve on the daily operation. They can provide the required share either through their own resources, through bilateral agreements with other market participants, or by participating in the market [78].

Many ISOs in the US send the requirement of spinning reserve share to the market participants before the day ahead market happens. For instance in ERCOT, before the DAM for each day d, at 6 am on day $d-1$ ERCOT assigns part of the ancillary service plan quantity, by service, by an hour, to each load-serving entity (LSE) based on its load ratio share during the past seven days. Aggregators participate in the market on behalf of the LSE and they are responsible for providing spinning reserve by any of the three above-mentioned methods. Fig. 3.2 shows the timeline of events in ERCOT. Qualified scheduling entities (QSE) are eligible market participants in the day

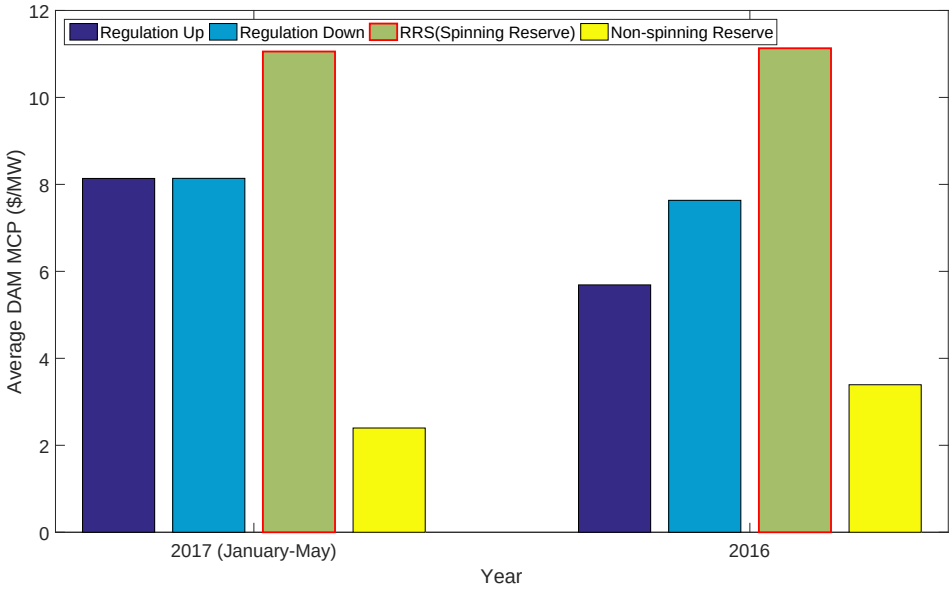

Figure 3.1: The average prices of different ancillary service products in ERCOT.

ahead and real-time market in ERCOT.

For an aggregator to qualify the provision of certain ancillary services, several key questions need to be addressed. First, how does ISO certify the resource for ancillary service? Second, what happens at the spinning reserve deployment time? Third, What happens after the recall of deployment? and Fourth, What happens if aggregator failed to provide its spinning reserve share to the market? In the next section, we present the framework of the proposed concept.

3.2.1 How ERCOT qualifies a resource to provide spinning reserve?

Before ERCOT let QSE participate a load resource into the market, a test will be performed. During this test period, QSE should be able to update its ancillary service plan every 15 seconds. Once a basepoint is given by ERCOT, QSE has 10 minutes time to reach the base point. For load resources participating as RRS, after 10 minutes, the base point of them $must$ be between: a)The resources RRS capacity or b)The requested deployment. QSE can request ERCOT to perform this test at the aggregation level instead of individual-level [71]. The importance of the last point will be discussed in 3.4.2 and 3.6.1.

3.2.2 What happens at the deployment time?

Upon an event, a new base point will be sent to QSEs in the next SCED cycle. After getting deployed, QSE must update the RRS schedule for its generators and controllable loads within one minute (announce their deployment amount) [71].

3.2.3 What happens after the recall of deployment?

ERCOT monitors and reports non-compliance to Texas Regional Entity(TRE) within 24 hours. Two failures to follow ERCOT RRS deployment signal can disqualify the load resource from providing RRS. Six months after disqualification, the load resource can re-apply and pass the tests again [71].

3.2.4 What happens if QSE fails to provide its share?

The load resources should be available to provide spinning reserve within 3 hours of the recall of spinning reserve deployment signal. If load resources are unable to provide their obligation after this three hours window, QSE should replace them trough other generation resources during these hours [71].

3.3 Conceptual Analysis of Benefits for Consumers, Aggregators and the ISO

This section offers a conceptual analysis of a possible dominant strategy that benefits the three major stakeholders in this process, namely, the end users, the aggregator, and the ISO.

3.3.1 Benefits for end users

Pumps circulate the water through a filter and a chlorinator. Maintaining the chlorine level of the water is an important part of maintaining healthy pool water. Too much chlorine causes skin and eye irritation. Too low chlorine speeds the formation of algae and causes the water to look cloudy and green. Besides health issues, keeping the pool cleaned is essential to maintain the residential pool permit [79]. Therefore pool owners need to turn their pool pumps {ON} for a certain number of hours every day.

Sunlight, the temperature of water and amount of bacteria in the water have a direct correlation

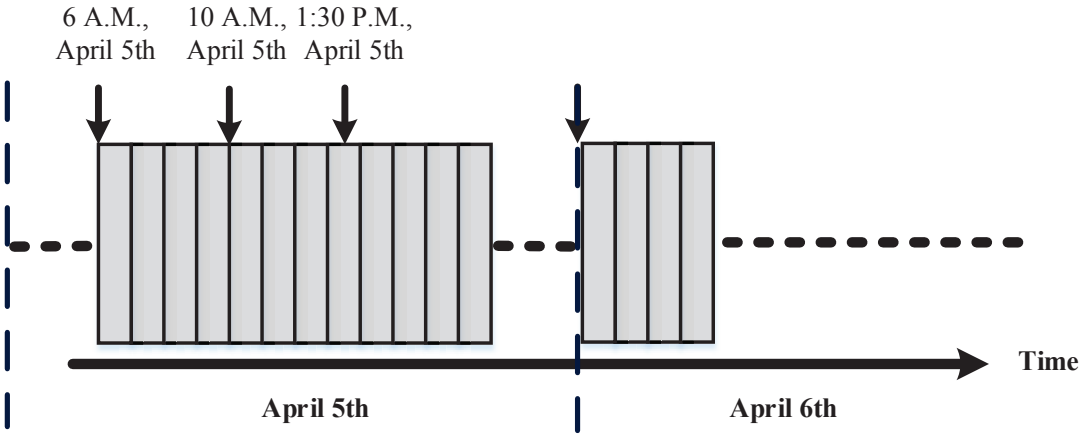

Figure 3.2: At 6 a.m., ERCOT publishes ancillary service plan for each QSE for the next day. This plan identifies the ancillary service obligation for all QSEs in each hour. At 10 am, ERCOT starts the Day-Ahead Market for April 6th based on bids/offers received for energy/reserve for each hour of April 6th. At 1:30 pm, ERCOT closes the day ahead energy and ancillary service market for April 6th and publishes the results.

to the water's ability to maintain its chlorine level. On a hot sunny Saturday, most swimming pool pumps need to circulate water for their whole cleaning cycle, *e.g.* for around 12 hours [80]. However, on a cold Monday, not much pool pumping is needed and pool water maintains its chlorine level. If the same full cycle pumping happens for this day, the chlorine content of the pools can reach an unhealthy level.

Keeping the pool water quality within the healthy margin is a burden for the pool owners. Upon questioning some of the pool owners, we found some turn {ON} the pool pump for the entire weekend only, and some invest and buy a timer to turn {ON} the pump for a certain number of hours every day and they adjust the timer based on the season. The first approach can result in the pool water reaching the over-cleaned status and the chlorine level can go above the healthy margin at the end of the weekend. Since water maintains it chlorine level during the cloudy days, a fixed number of cleaning hours can also cause over/under cleaning for days with different weather conditions.

Centralizing this control can enhance the comfort of the customers by automatically changing

the number of required cleaning hours each day based on the weather forecast. There is also a room to save money for customers with optimal activation of the pumps. Also, since the communication with the smart switches is bi-directional, in the case of a switch failure, the aggregator will be informed to replace the switch.

3.3.2 Benefits for aggregators

Due to health and license concerns mentioned above, swimming pool pumps are *must-run* loads. However, there is flexibility in the time of the day to run these demands. If aggregators equip the pools in an area with Wi-Fi enabled {ON,OFF} switches and be able to reliably control them, they can gain benefits by providing a part of their (possible) ancillary service mandate using pools, and potentially participate in the spinning reserve market while controlling considerable energy consumption of their resources. Capital investment and benefits gained from this investment are key concerns and will be addressed in this Chapter. It will be shown in Section 3.6 that given the spinning reserve prices in ERCOT, and only by investment in one city in ERCOT region, aggregators can return their investment capital in less than a year, and gain a profit as high as \$1M/year afterward.

3.3.3 Benefits for the ISO

Maximizing social welfare while keeping the system secure is one of the main objectives of ISOs. Normally, a certain capacity of generators is dedicated to providing spinning reserve. It can be shown that reducing the generators' capacity commitment to spinning reserves could increase social welfare. A simple example of this situation is shown in Fig 3.3. Suppose three units where one of them (unit B) can provide spinning reserve. As can be seen Fig 3.3, dropping this requirement decreases marker clearing price and increases the social welfare.

The second advantage of such a reserve comparing to acquiring reserve from conventional generators or big industrial loads is its geographical diversity which is quite desirable during contingencies.

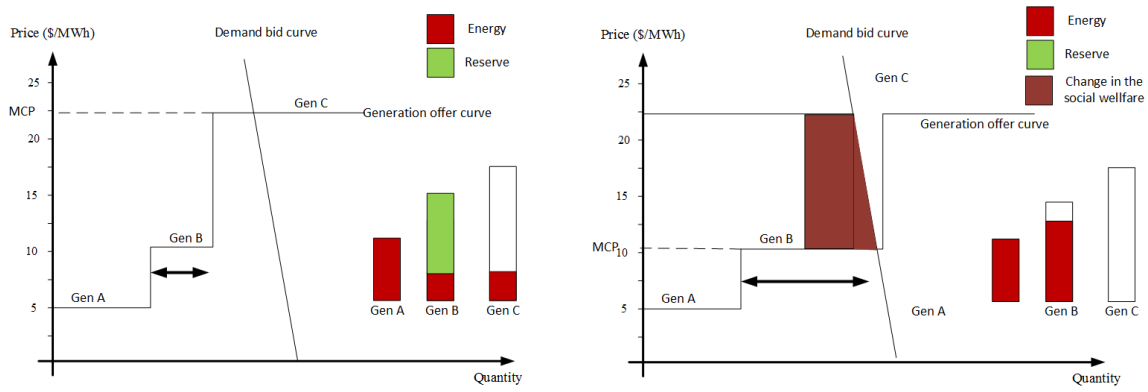

Figure 3.3: An example of the increase in the social welfare when units with lower marginal cost can provide more energy instead of holding a certain capacity as reserve. Left: part of the capacity of Gen B cannot be used due to the need for this unit capacity for spinning reserve. Right: Spinning reserve was provided from another source letting this unit to produce more, and lower the market clearing price (MCP).

3.4 Reliable Reserves from Pool Pumps

In this section, we present the methodology of firming up reliable reserve (defined in ISO's terms) from the aggregation of many controllable swimming pools. We describe the control method, the reliability assessment method, and the conceptual equivalence to large power plants.

3.4.1 Control strategy for pool pumps

Centralized direct load control is used to control the pool pumps participating in the program. The direct control will be through installing a Wi-Fi enabled {ON,OFF} switch exclusively for the pool pump. Some examples of commercial {ON,OFF} switches compatible with the proposed method are [81–83], along with many other brands. Their prices typically vary from $5-$50 [84] depending on the robustness of embedded software, power rating, and features such as connectivity to other smart home appliances [85].

As discussed in Section 3.3, pool pumps are located outside the homes and they only need to turn {ON} for a certain number of hours. Therefore, the privacy of customers will not be violated with a centralized control scheme. At the deployment time, after ISO send deployment signal to the aggregator, aggregator updates base points for its resources within a minute. For instance in

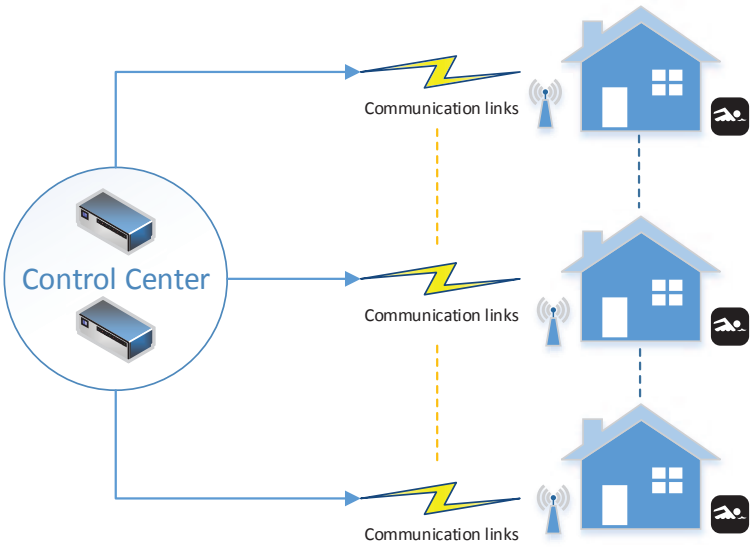

Figure 3.4: A schematic of system architecture being used.

ERCOT, QSE is required to reach 95% of this base point within ten minutes. Since communication between the IoT switch and the control center happens in real time every few seconds, 9 minutes is more than enough time to get 95% required response. In the next subsection, the feasibility is discussed.

3.4.2 Capacity credit of pool pumps

Capacity credit of swimming pool pumps can be defined as the MW capacity equivalent of pools aggregation to 1 MW capacity from a conventional power plant. A reliability assessment of the control and communication network of swimming pool pumps is needed to find the capacity credit of swimming pools. For that purpose, it is essential to know the connectivity structure of the components in the system. The schematic of the system architecture used in this Chapter is shown in Fig. 3.4 [86]. In engineering systems, components are connected in parallel, series, meshed or combination of these [87].

The system being studied normally consists of two control centers (aggregator or QSE), various communication links between the control center and the wireless network of each house, the switch controlling swimming pool pump and the pump itself. Series/parallel structure of the mentioned

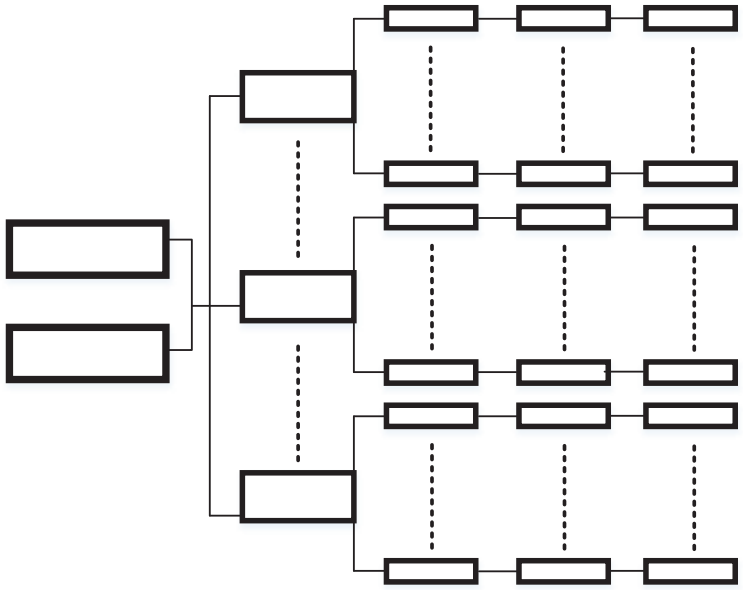

Figure 3.5: Series/paralleled structure of pool pump control system.

components is illustrated in Fig. 3.5. Pump, switch, and the home wireless network is in series with each other. A set of homes using the same Internet provider/cable are in parallel with each other. The same series/parallel trend happens until the control center. Since control centers, modern communication networks, and pool pump itself are highly reliable components, without loss of generality, in this Chapter failures are only considered in-house wireless networks and pool pump switches, considering other components as fully reliable.

Hazard rate or failure rate of a component is defined as the ratio between the number of components failed in an interval and the average number of components survived in that period [87, 88]. It can be estimated with a replacement test as the ratio of failures to the component hours accumulated. A typical hazard rate curve of an electrical component is shown in Fig. 3.6. Due to its shape, this figure is normally referred to as bath-tub curve. Bath-tub curve consists of three major parts. In region I, hazard rate decreases as time passes due to a decrease in the possibility of factory errors. In region II, the failure rate is constant, and the component is in its useful life period. In region III, the failure rate starts to increase. It happens when a component exceeds its useful lifetime and should be replaced. More details about bath-tub curve and the useful lifetime

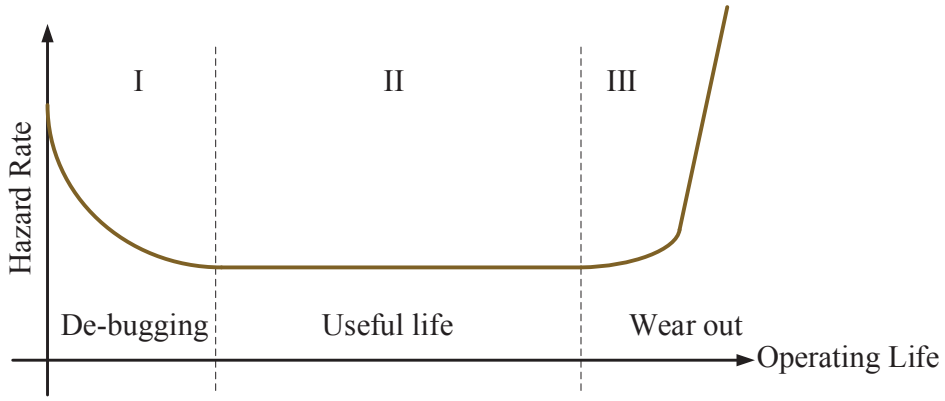

Figure 3.6: Typical hazard rate of an electrical component as a function of its age.

of a component can be found in [89, 90]. In this Chapter, components are in their constant hazard rate lifetime, and being replaced afterward. Therefore λ and μ are fixed.

3.4.2.1 Simple state space diagram

State space diagram of each customer participating in this program is shown in Fig. 3.7. For a Wi-Fi+modem and an {ON,OFF} switch with failure and repair rate (λ_w, μ_w and λ_s, μ_s in Fig. 3.7 respectively), probability of each pump residing in up mode can be calculated using frequency and duration method showed in [87, 88]. Therefore, the accessibility of each pool pump in a house can be calculated as (3.1). In this work, the type of all switches an LSE uses to control its customer's pool pumps are assumed to be identical. Also, wireless network in all houses is assumed to have the same failure rate and repair time.

$$P_{mode_A} = \frac{\mu_s \mu_w}{(\lambda_s + \mu_s)(\lambda_w + \mu_w)} \tag{3.1}$$

Since each pool is accessible (controllable) with probability P_{mode_A} and it is unavailable with probability $1 - P_{mode_A}$, and individual pools are independent of each other, to find the Probability Density Function (PDF) of the total number of available pools, we can use Binomial distribution. For instance using (3.1) and $\lambda_w = \frac{1}{99} f/hr, \mu_w = 1r/hr$ and $\lambda_s = \frac{1}{9} f/hr, \mu_s = 1r/hr$ and $N_{pools} = 34122$, PDF of accessibility of k pools can be drawn as Fig. 3.8. The probability of

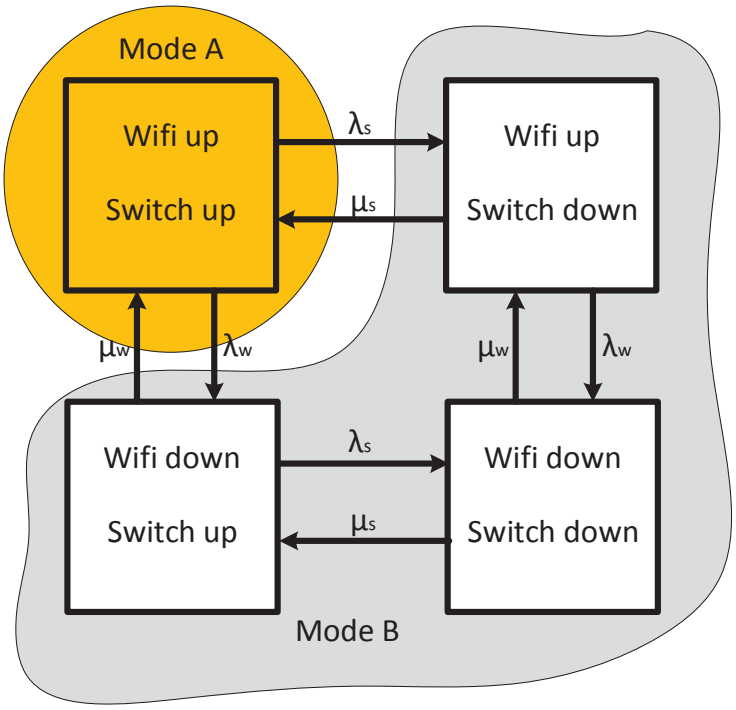

Figure 3.7: State space diagram for a two-component system: Mode A: Pool pump is accessible for the reserve market, Mode B: Pool pump is not accessible for the reserve market.

getting exactly k pools responsible for the reserve market is $\binom{N_{pools}}{k}(P_{mode_A})^k(1-P_{mode_A})^{N_{pools}-k}$. ERCOT requires at least 95% of base point in 10 minutes [71]. Assuming that all pool pumps consume the same amount of electricity while on {ON} status, to find the equivalent number of pools, the inverse Binomial probability distribution can be used. This is the level that is qualified for participation/procurement in the ERCOT market. For this example, this level is shown by green dashed line in Fig. 3.8.

3.4.2.2 Detailed state space diagram

In subsection 3.4.2.1, some customer related factors were ignored. First, there should be a dynamic rate of disabling for each individual pool pump. Upon our field study and interviews with pool owners, we realized they might not pay attention to their pool is controlled most of the days in a year, but on some days such as 4th of July which pool events are popular, there will be a higher potential to override our control and keep the pool in the ON state for the entire day. This rate

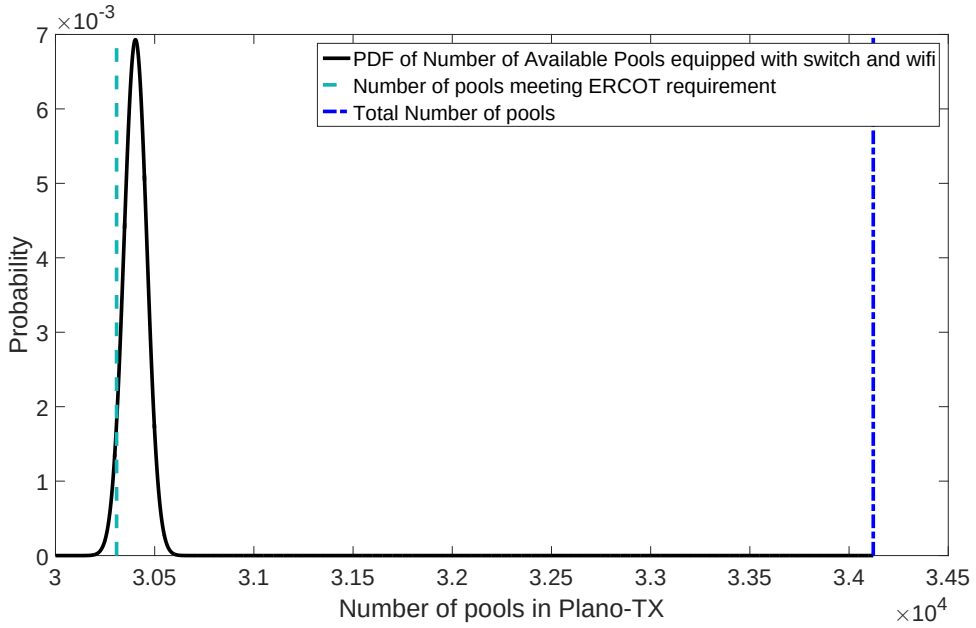

Figure 3.8: Illustration of qualified pools, and PDF of available pools.

should be added to the model and should be defined each day according to the possibility of such action. Such state is depicted as *disabled* state in Fig. 3.9. For a cold weekday, this rate could be extremely low and for a warm 4th of July, this rate would be higher. Estimating this rate requires a separate data analytic which can be a part of the future works.

Furthermore, the possibility of common mode failure should be added to the model in Fig. 3.7. In the previous section, the failures cannot be common between pool pump and control device, WiFi network. However, some events might trigger a common mode failure that both appliances are out of service immediately. Events such as disconnection on electricity supply. This was modeled in Fig. 3.9. There is a transition between both components in the ON mode suddenly going to OFF mode. However, no such transition should exist for the return to normal state.

Same as the previous Markov chain, there is a steady state probability of residing in each state at all times. However, the closed form parametric description of it might not be as clean and straightforward as (3.1). Therefore we use a typical approach to find the limiting probabilities based on [87]. This approach is based on the definition limiting probability: the probability of

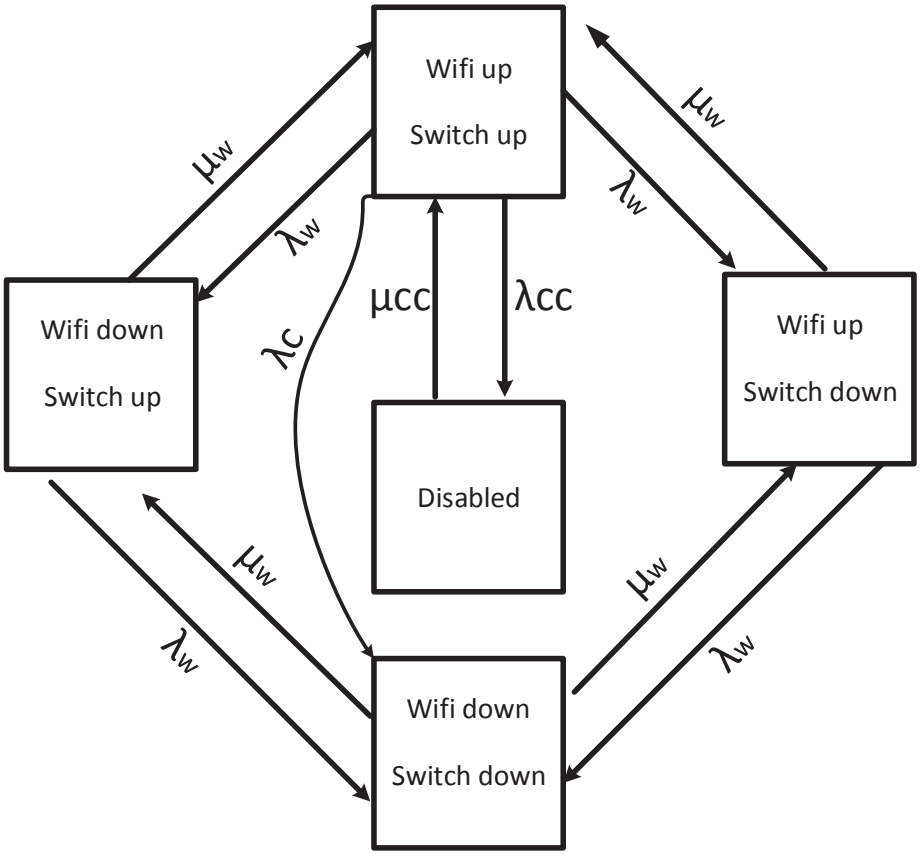

Figure 3.9: Illustration of more realistic Markov chain approach.

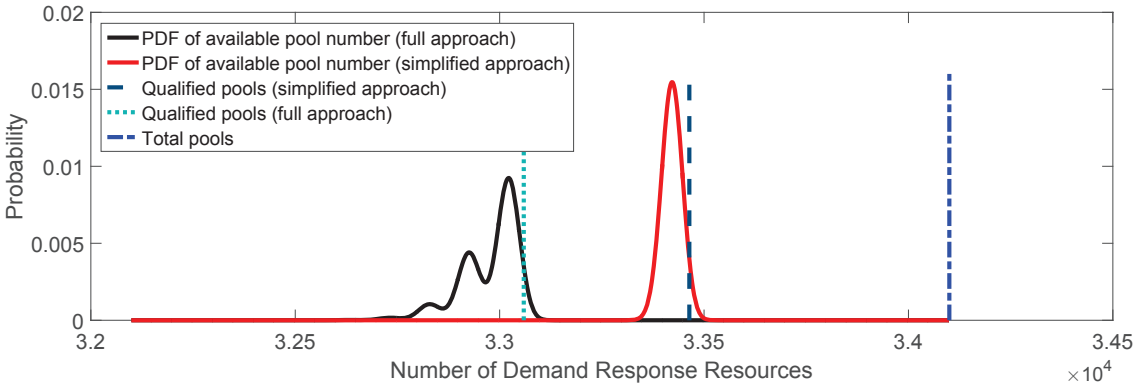

Figure 3.10: Different system level probability istributions and the impact on the qualified level to be participated into the wholesale market.

being in each state would not change after one additional iteration around that state. The equation in (3.2) gives five dependent equations and can be solved by discarding one of them and replacing it with $\sum_{i=1}^{n} P_i = 1$. P is a row vector stochastic transitional probability matrix, and α is the limiting probability of residing in each state.

$$\alpha \times P = \alpha \tag{3.2}$$

3.4.2.3 Impact of ISP failure

Internet service providers are very unlikely to fail. However, to study their impact we considered their individual failure rate and repair time and built the Capacity Outage Probability Table (COPT) accordingly. After such procedure, the system-wide COPT can be attained by performing convolution overall individual ISP COPTs. Essentially a summation over probability distributions is being performed.

Fig. shows the changes to the individual probability distribution and Fig. shows how system-level PDF varies after such change. It should be noted that parameters are pessimistically selected to show the changes visually and in reality, ISPs are having a low failure rate and incredibly fast repair time that the changes might be insignificant.

Approaches described in subsections 3.4.2.1 and 3.4.2.2 are two ways to find the capacity can

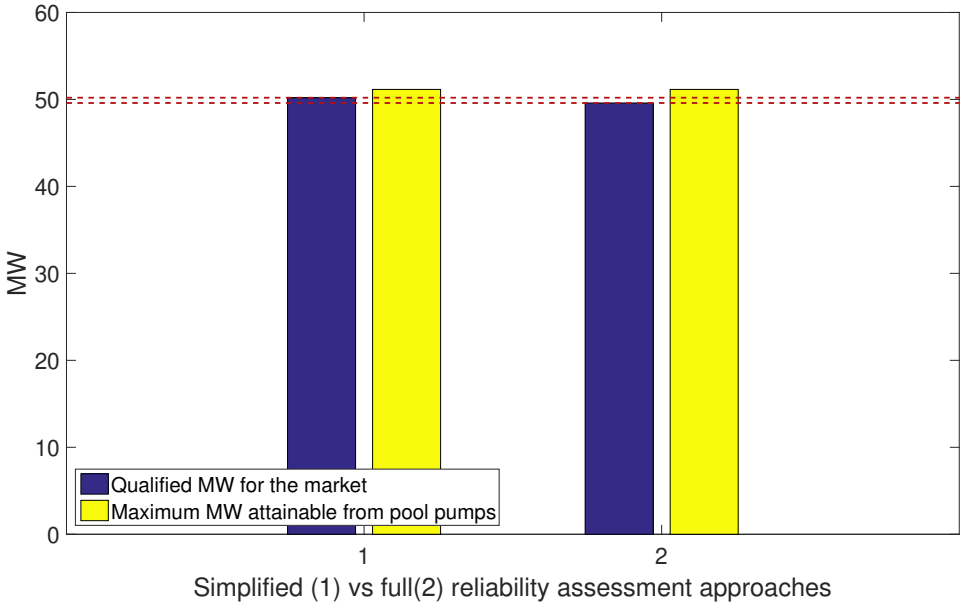

Figure 3.11: Changes in qualified capacity using detailed and simple approaches.

be participated in the market. In the following sections, we consider the operational planning procedure given this capacity. In other words, this capacity will be defined well before the day-ahead market opens for the day mainly according to the weather forecast, and customer behavioral forecast. We used results from the simple approach in the following sections, while it can be adapted for the full version with minimal changes.

3.5 Scheduling the Pool Pumps for Operational Planning

Based on the discussion in the previous section, in this section, we discuss how to schedule pools for each hour of the day. From Section 3.4.2, we have $sr^{pools}[t] = f(u[t])$, where $u[t]$ is the aggregated MW of pools capacity and $f(u[t])$ maps capacity of pools to their capacity credit, $sr^{pools}[t]$. $sr^{pools}[t]$ should be chosen such that for the entire day it minimizes the cost of the aggregator in procuring energy to serve pools and reserve from the DAM when desirable. Therefore, a co-optimization of energy (that is going to serve part of the reserve) and reserve (from the DAM) is needed to find the best operating plan for the aggregator.

Since in this stage a decision is going to be made on the {ON,OFF} statuses of pool pumps

for each hour of the next day, we potentially face with $24 \times N_{pools}$ integer variables in the optimization problem. However, assuming that all pool pumps consume 1.5 kW, we can use the relaxation method used in [91], and solve for the total MW from pools, knowing that $u[t] = 1.5 \times 10^{-3} \sum_{p=1}^{N_{pools}} p_i[t]$, where $\{p_i[t] \in \{0,1\}\}$ is the {ON,OFF} status of individual pool pumps and N_{pools} is the total number of pools under control. After $u[t]$ for all hours schedules, it will be distributed among the pools.

3.5.1 Deterministic bidding approach

This process happens after aggregator received its obligation in providing spinning reserve for each hour of the next day, $SR^{req}[t]$, at 6 am on day $d-1$ in Fig. 3.2. Also by this time, the number of hours pools need to be cleaned on the next day, $\mathcal{H}_d^{req}$ is defined based on discussion in Section 3.3. The deterministic optimization that tells aggregator how to schedule its pool pumps and how much reserve to purchase from the DAM is as (3.3). $\pi^E[t]$ and $\pi^R[t]$ in (3.3a) are forecasted DAM energy and reserve prices. $f(u[t])$ is the function maps capacity to capacity credit comes from Section 3.4.2. It will be shown that for the structure of this problem, it can be written as $f(u[t]) = \frac{1}{\mathcal{D}} u[t]$ where $\frac{1}{\mathcal{D}} \leq 1$ is the estimated degrading factor. In case that all components in the system are fully reliable, $\mathcal{D} = 1$. (3.3b) ensures aggregator complies with the ISO requirement. (3.3c) ensures pools are being cleaned the minimum required number of hours every day. $\mathcal{H}_d^{req}$ and $\mathcal{H}_d^{max}$ are the required and maximum number of hours each pool pump should circulate water per day d and $U^{max} = 1.5 \times 10^{-3} N_{pools}$ is the maximum MW capacity from swimming pools equipped with required devices. Constrains (3.3d) ensures the capacity of pools scheduled to be {ON} does not exceeds the maximum capacity of pools combined.

$$\min_{u[t],sr^{DAM}[t]} \quad \sum_{t=1}^{T=24} \pi^{E}[t]u[t] + \pi^{R}[t]sr^{DAM}[t] \tag{3.3a}$$

$$s.t. \quad \frac{1}{\mathcal{D}}u[t] + sr^{DAM}[t] \geq SR^{req}[t] \quad \forall t \tag{3.3b}$$

$$\mathcal{H}_d^{max}U^{max} \geq \sum_{t=0}^{24} u[t] \geq \mathcal{H}_d^{req}U^{max} \tag{3.3c}$$

$$0 \leq u[t] \leq U^{max} \quad \forall t \tag{3.3d}$$

We showed the deterministic formulation of our problem. However, since the operational planning stage happens before the DAM, energy and reserve prices are yet to be known and uncertain. Therefore there is a need to manage this uncertainty in the planning problem. In our future work, we discuss our solution for this challenge through scenario approach optimization.

3.5.2 Scenario-based bidding approach

Since constraints in (3.3) are all deterministic constraints, they are remaining the same in the $(1-\epsilon)$ robust operational planning (scenario-based) formulation. However, the objective function tries to minimize the cost of operational planning for the worst realization of uncertainty among $\mathcal{S}$ scenarios. The objective function of our scenario problem is as (3.4).

$$\min_{\{u[t],sr^{DAM}[t]\}} \max_{\{\forall \delta_i \in \Delta_{\mathcal{S}}\}} \sum_{t=1}^{T=24} \pi_{\delta_i}^{E}[t]u[t] + \pi_{\delta_i}^{R}[t]sr^{DAM}[t] \tag{3.4}$$

Where $\Delta_{\mathcal{S}} = \{\delta_1, \delta_2, ..., \delta_{\mathcal{S}}\}$ are energy and reserve empirical samples of $\mathcal{S}$ days chosen randomly from the DAM results of previous days. If we rewrite this problem in epigraphic format, we can solve this problem as a linear programming one [92]. Full epigraphic formulation of the problem is as (3.5). (3.5b) is the only uncertain constraint in this problem and it will be violated with the probability of at most ϵ. Therefore, the realization cost for the decision made in (3.5) will not exceed h with $(1-\epsilon) \times (1-\beta)$ confidence. It should be noted that as ϵ goes to zero, the solution of scenario problem approaches the robust solution which might be too conservative,

while β can be chosen as a very small number, e.g. 10^{-10} without a big impact on the number of required scenarios as shown in (2.8).

$$\min_{\{u[t],sr^{DAM}[t],h\}} \quad h \tag{3.5a}$$

$$s.t. \quad \sum_{t=1}^{T=24} \pi^{E}_{\delta_i}[t]u[t] + \pi^{R}_{\delta_i}[t]sr^{DAM}[t] \leq h, \quad \forall t, \forall \delta_i \in \Delta_{\mathcal{S}} \tag{3.5b}$$

$$\frac{1}{\mathcal{D}}u[t] + sr^{DAM}[t] \geq SR^{req}[t] \quad \forall t \tag{3.5c}$$

$$\mathcal{H}^{max}_{d} U^{max} \geq \sum_{t=0}^{24} u[t] \geq \mathcal{H}^{req}_{d} U^{max} \tag{3.5d}$$

$$0 \leq u[t] \leq U^{max} \quad \forall t \tag{3.5e}$$

3.6 Case Study

This case study is performed based on data from Plano-Texas. Plano is located near Dallas in North Texas. The percentage of houses having swimming pools in this city is the 10th in the US and the highest in Texas. According to [93], 31% of houses in this city have a swimming pool (Google Earth view over this city can be seen in [94]). The list of other top 9 cities with private pool can be seen in Fig. 3.12 [93].

Using population and people per household data in [95], the number of swimming pools is estimated as 34122 pools. The assumption in this case study is that all participating pools are the same size, equipped with $1.5kW$ pool pump. Therefore, it gives the aggregator a maximum total capacity of 51.183 MW, 4-12 hours per day. However, based on Subsection 3.4.2, not all of this capacity is qualified for scheduling. First in 3.6.1, we discuss reliability assessment of three different investment strategies, then in 3.6.2 results of the operational planning stage based on formulation in 3.5.1 will be compared. A discussion on the cost-benefit analysis of three investment cases will be performed in 3.6.3.

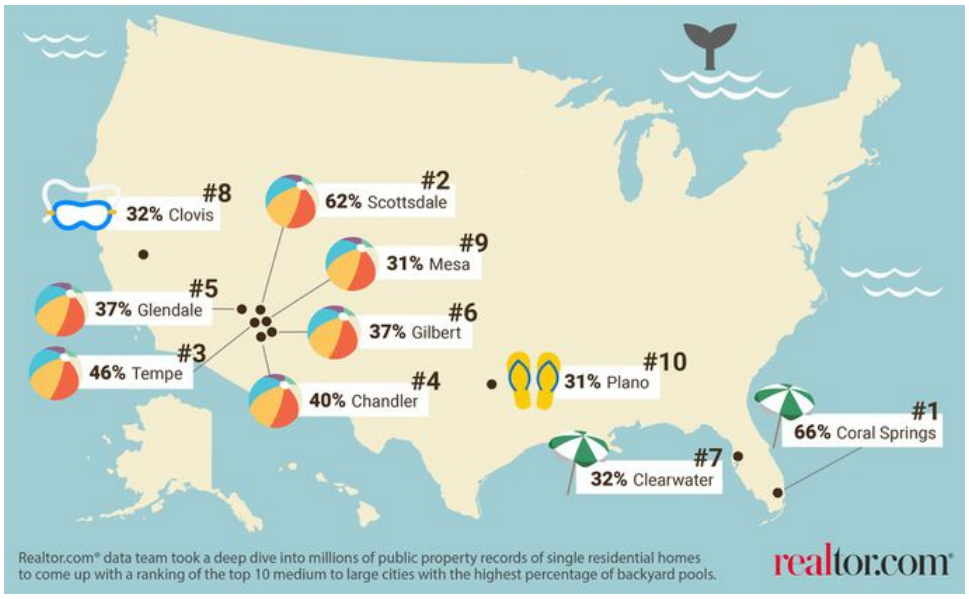

Figure 3.12: Top 10 Cities with Pool-Loving Homeowners in the US.

3.6.1 Reliability assessment

According to the discussion in Section 3.4.2, failures are considered for the wireless network and {ON,OFF} switches. It is assumed that all houses in this case study affluent enough to have a private pool, already equipped with a Wi-Fi network. Failure rate and repair time of the Wi-Fi network in these houses are shown in Table 3.1. Also, it was assumed that Wi-Fi network in these houses being maintained by their owners and its failure rate always resides in region II of Fig. 3.6.

Three different strategies were considered to invest on the {ON,OFF} switch installation. A very reliable switch with 10 years useful life and nominal rating of $1.8kW$ (switch type 1) [81]. A reliable switch with the same rating [83] and 5 years nominal life (switch type 2), and a basic switch with a nominal rating of $1.5kW$ [82] and with three years average life in region II of Fig. 3.6 (switch type 3). It should be emphasized that numbers in Table. 3.1 are indicative and not factory announced data. Also, a failure in the switch is considered as a failure of the switch software in accurately following the orders from the Wi-Fi network and not the switch hardware itself.

Following the procedure in Section 3.4.2 and using the data in Table 3.1 for each investment pattern, P_{mode_A} can be calculated as shown in Table 3.2. The percentage of available pools as

Table 3.1: Reliability parameters of components

Component	Region II Width (years)	λ (failure/hr)	μ(repair/hr)
Wi-Fi	N.A.	$\frac{1}{99}$	1
Switch Type 1	10	$\frac{1}{999}$	1
Switch Type 2	5	$\frac{1}{99}$	1
Switch Type 3	3	$\frac{1}{9}$	1

a function of the number of pools is as shown in Fig. 3.13. There will be a steep drop in the percentage of usable pools capacity for the reserve market if the number of pools participating in the program is not big enough (e.g. < 1000 pools). Capacity credit as a function of participated capacity is shown in Fig. 3.14. As can be seen, this function can be represented as a linear function, $f_{(x)} = \frac{1}{\mathcal{D}}x$ as was used in the operational planning stage formulation.

For the number of pools in Plano, the estimated $\mathcal{D}$ is available in Table 3.2. As can be seen, selecting a cheap switch causes a higher $\mathcal{D}$ and in turn higher cost of energy in (3.3) and lower qualified reserve in (3.3b). Therefore selecting the right switch will affect the daily cost/benefit of the aggregator.

In the next section, we demonstrate the operational planning stage. To avoid redundant discussions, we fix the switch implemented in the system to the type 3 in this section. In 3.6.3, the summary of results using all three approaches are summarized.

Table 3.2: Reliability assessment results

Investment	Type 1	Type 2	Type 3
P_{mode_A}	$999 \times 99/100000$	$99 \times 99/10000$	$9 \times 99/1000$
$\mathcal{D}$	1.0121	1.0216	1.1258

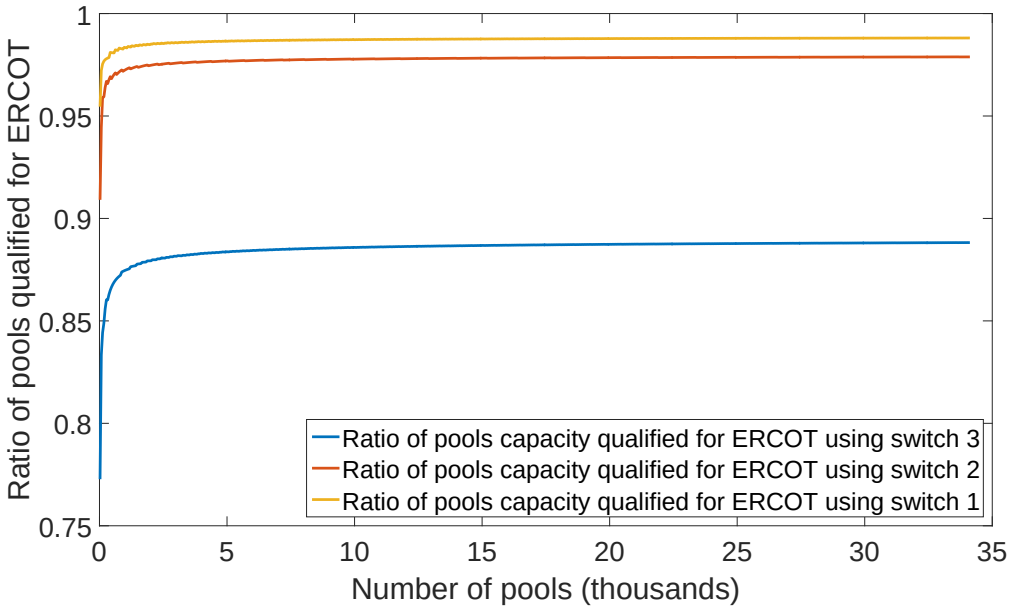

Figure 3.13: The correlation between the number of participating pools numbers and the ratio of useful spinning reserve for the market:$\mathcal{D}$ is very high for small, (e.g. < 1000) number of pools.

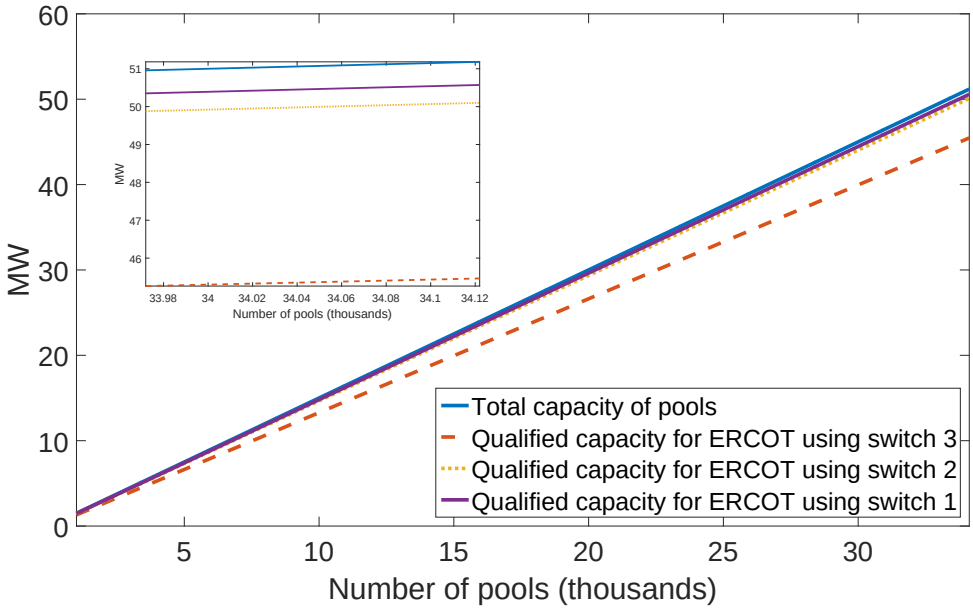

Figure 3.14: The relationship between the number of participating pools and the reliable provision of spinning reserves.

3.6.2 Bidding the pools into the market

In this section we show the market participation results. ERCOT spinning reserve requirement used in this section is based on May 27 requirement available in [96], normalized to the population of Plano-TX. As can be seen by yellow dashed lines in Figs. 3.15,3.18, ERCOT reduces the requirement during the day due to low wind forecast and lower uncertainty during these hours. Price samples were extracted for January-April of the past five years. Two different pool pumping scenarios considered in this section. One is for the times that potential of algae production is high according to the discussion in Section 3.3. Therefore there will be a need to pass the entire water of the pool through the chlorination to increase the chlorine content of the water. The other day is a day that not much filtration is needed.

3.6.2.1 A hot sunny Saturday

In this scenario, the aggregator sees the forecasts of day-ahead that has a big potential for algae production, because Saturday is going to be a sunny, warm and high pool usage potential. Therefore the decision will be to operate pool pumps for the full cycle, 12 hours. $\mathcal{H}_d^{req}$ and $\mathcal{H}_d^{max}$ are set to 12 and 14 respectively. The operational planning results are shown in Figs. 3.15 and 3.16. Big statistical savings also acheived by using scenario approach formulation as seen in Fig. 3.20. 440 days of price points from ERCOT was used in the scenario program simulation. Given the number of samples and $d = 49$, $(24 \times 2 + 1)$, with $\beta = 10^{-6}$, $\epsilon = 0.1976$ using results of Theorem 1 in Chapter 2. It should be noted that while using more data is desirable, the possibility of the samples not having identical underlying distribution gets higher as we collect data further away from the past. Therefore as more data gets collected possibility of *bad* samples get higher and a need for a proxy to make raw data identically distributed rises.

3.6.2.2 A cloudy cold Monday

In this scenario, aggregator day-ahead forecast shows a cloudy colder than usual Mondays in Plano. Therefore it decides *not* to operate its controlled pool pumps for the whole 12-hour cycle. It is due to the fact that the main cause of a reduction in the chlorine content of water, bacteria,

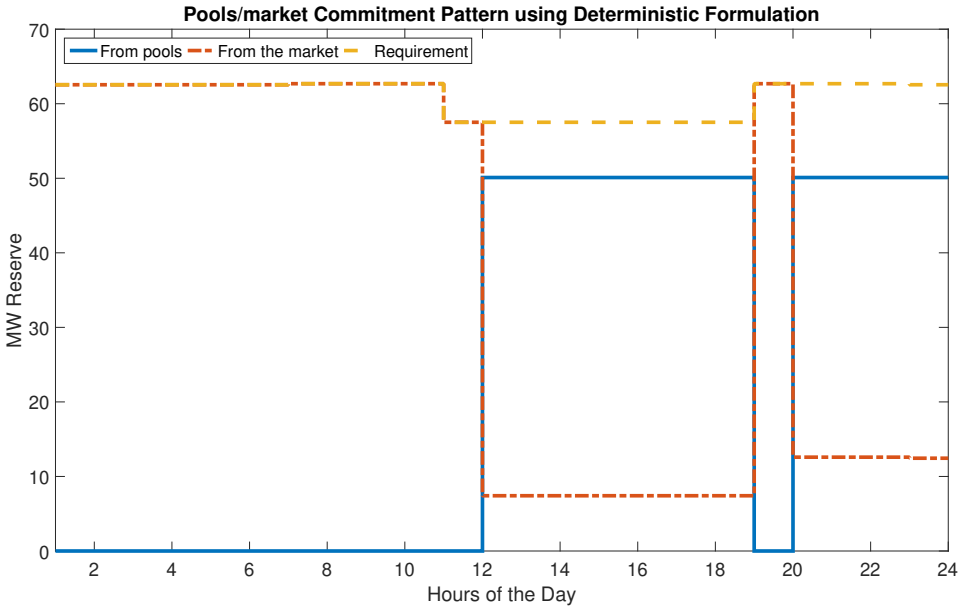

Figure 3.15: Operational planning results using the deterministic formulation: A hot sunny Saturday.

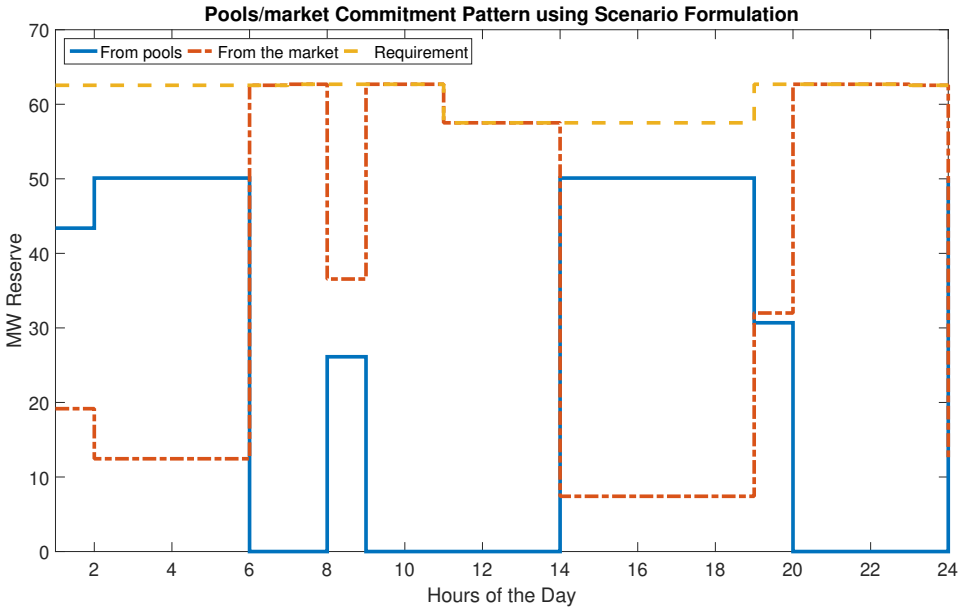

Figure 3.16: Operational planning results using the scenario formulation: A hot sunny Saturday.

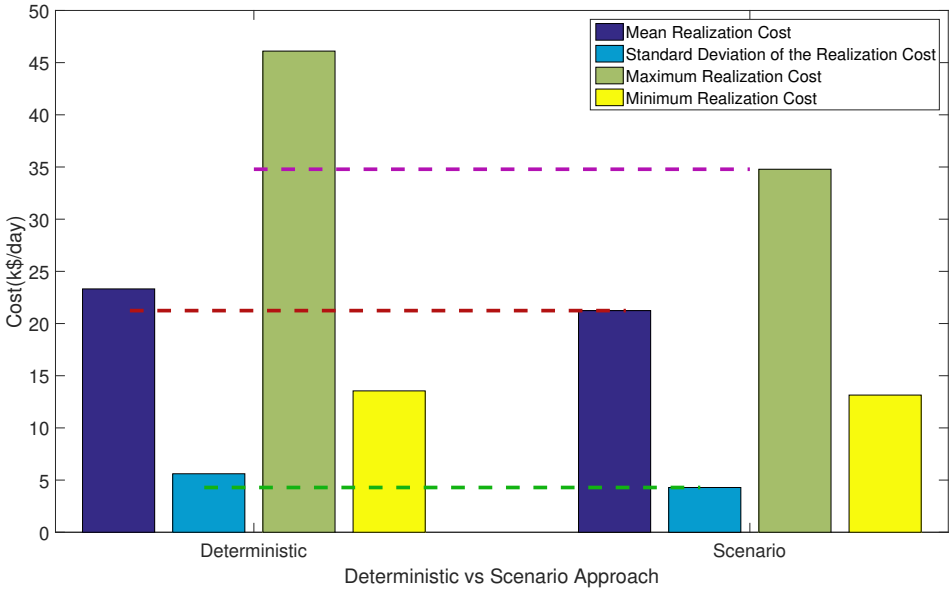

Figure 3.17: Comparison of the finantial results using the scenario and deterministic approaches: savings are clear in all statistical aspects of the results.

and sunlight, and indirectly water temperature, are at a low level. Operational planning results can be found in Figs. 3.18 and 3.19. $\mathcal{H}_d^{req}$ and $\mathcal{H}_d^{max}$ are set to four and six respectively. The scenario approach hedges against the uncertainty in the price so as illustrated in Fig. 3.20 on average it saved money and reduced the statistical variations in the profit margins.

It should be noted that to know the exact upper bound on the violation probability for our scenario results, the data needs to pass the IID test. Since this chapter unlike Chapter 2 we used raw data, we do not claim any risk related results. However, generating the IID data from raw data is an active line of research within our co-authors in [8].

3.6.3 Cost-benefit analysis

Two sets of cost-benefit analysis have been done in this subsection. First, we consider one city and assume that we attract all customers in that city to the plan and we consider three types of investments but with one average weather scenario. In the second analysis first, we consider 1-10% customer procurement and second, we consider three different weather scenario and their

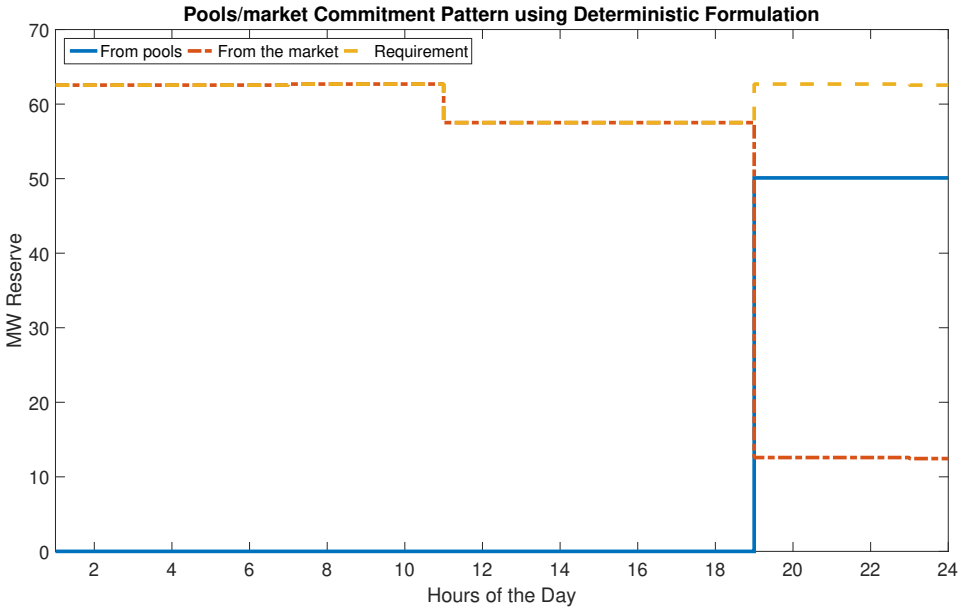

Figure 3.18: Operational planning results using the deterministic formulation: A cloudy cold Monday.

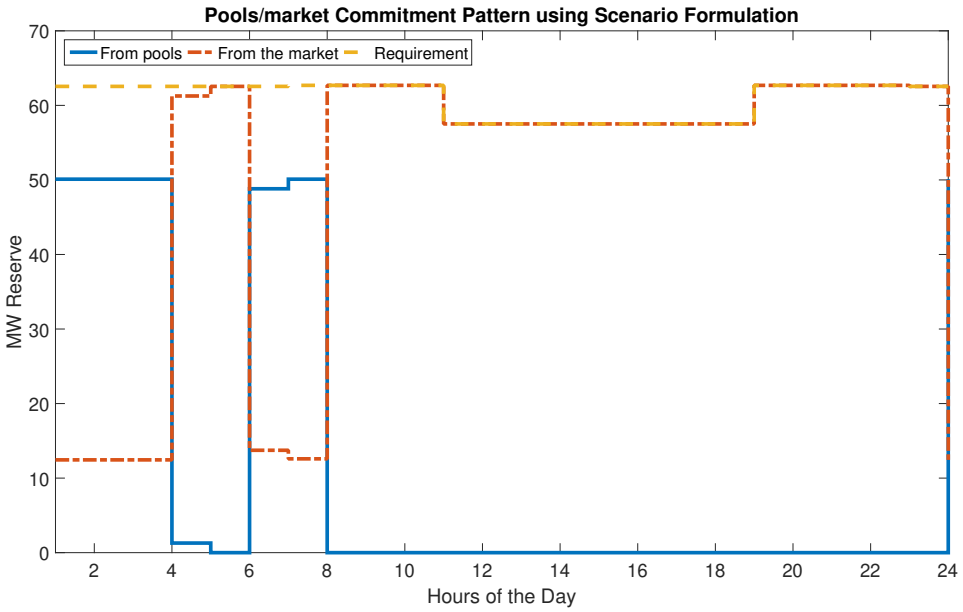

Figure 3.19: Operational planning results using the scenario formulation: e.g. A cloudy cold Monday.

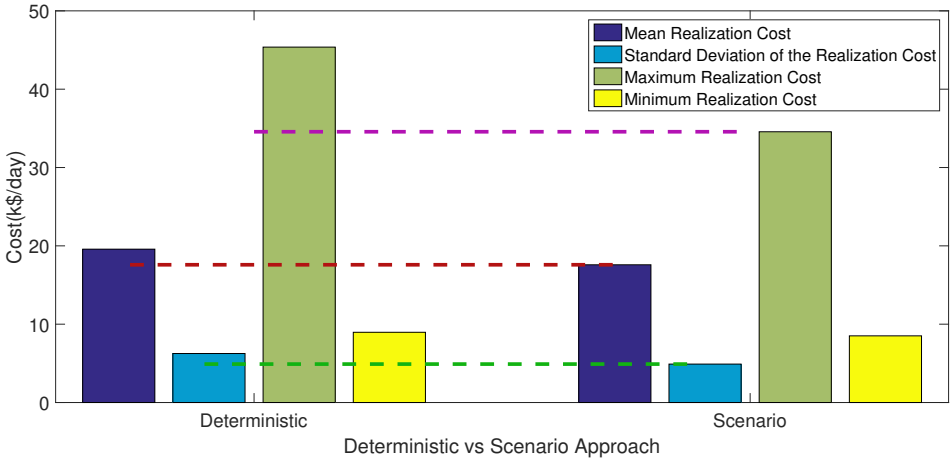

Figure 3.20: Comparison of the finantial results using the scenario and deterministic approaches: savings are clear in all statistical aspects of the results.

annual profit outcome.

3.6.3.1 Cost-benefit analysis: impact of investment strategy in pools in Plano-TX

The cost-benefit analysis is done by using historical spinning reserve price in ERCOT for the first four months of 2017. Three mentioned switch investment cost is considered along with one time $1 million flat upfront investment cost (other than the cost of switches). This cost should cover organizational costs needed for the aggregation strategy mentioned in this work. The study for all investment strategies was performed over a span of 10 years. Switches are being replaced after their lifetime. Average cleaning of 8 hours per day is assumed. As can be seen in Table 3.3, the net present value for the cheapest switch is less than other investment strategies due to worse degrading factor and recurrent investment cost over the 10 years span. Switch 1, however, has the highest net present value, although it has the highest investment cost. Considering the fact that the lifetime of this switch is the highest among all three switches, it leads to the highest net present value for an investment. The results of the net present value analysis in Table 3.3 are based on 5% interest rate for the entire 10 years study period. Given the assumption above, type 1 switch is the best investment strategy.

It should be noted that some other factors might affect the results in Table 3.3. Factors such as:

Table 3.3: Cost benefits analysis results: $1 million flat upfront organizational cost (other than the cost of switches) applied to all cases

Investment	Type 1	Type 2	Type 3
Cost Per Switch ($)	30	15	5
Annual Profit (M)	1.51	1.37	1.21
Net Present Value (M)	10.30	9.26	8.19

different average cleaning hours resulting from higher or lower number of days with cold weather for the city under investigation, different reserve prices for regions other than ERCOT, as well as possible installation costs. Future work will consider the impact of the price uncertainty on the performance of the investment.

3.6.3.2 Cost-benefit analysis: imact of weather scenarios on the profit

Type 1 of the investment was selected in this section and energy arbitrage is also considered in the profit calculation according to deterministic energy price forecasts.

If we simply divide the days of the year into three categories as below, the number of days per year that pools need each of the itemized cleaning cycles remains uncertain. In other words, weather pattern changes between years and therefore the optimal number of hours pool pumps are required to operate changes as well. To consider the weather scenario impacts we use three weather state that each day of the year will belong to one of them and three annual weather scenarios, assuming that each day in a year will lie somewhere among these scenarios. A summary of these state and scenarios are shown below and in Table 3.4.

- State 1 Days that full water circulation is needed (12-14 hours)
- State 2 Days that medium water circulation is needed (8-10 hours)
- State 3 Days that low water circulation is needed (4-6 hours)

Furthermore, we split the two sources of profit: profit from flexibility in the energy market or energy arbitrage and profit gained from the participation into the reserve market as illustrated in

Table 3.4: Three scenarios for a typical year.

Number of days in	State 1	State 2	State 3
Scenario 1	90	180	95
Scenario 2	45	180	140
Scenario 3	45	205	115

3.21. One other dirrerence with the simpler cost benefit analysis is optimal decision for each day based of the scenario approach formulation and previous scenarios.

As can be seen, the major source of profit comes from the participation in the reserve market, for the case of Texas. However, the utility can benefit from scheduling the pools on lower energy cost hours *and* higher reserve cost. A data analytics in the electricity trader's section should come up with these hours according to operational planning structure showed in Section 3.5.2.

The other factor being considered is the installation cost for each switch. For type 2 switch investment strategy we assumed $\$35$ installation cost per switch plus the flat $\$15$ switch cost making each house with pool cost a total of $\$50$. For 10 year operation with the assumption of price scenarios are valid for 10 years the net present value is $\$16.2M$ for 34100 pools in the city of Plano.

It should be noted that long term price forecast for energy and spinning reserve is not possible without in-depth knowledge on the network parameters and future generation plan and the prices used in this section was extracted based on the historical data on the spinning reserve price and energy price at the energy hub of Plano-TX. Therefore the net present values stated above are for illustration purposes only without loss of generality.

3.7 Conclusion and Expected Future Works

We propose a control strategy, reliability assessment and operational planning framework for an aggregator to control the swimming pool pumps and utilize their capacity credit for the provision of spinning reserves in wholesale markets. It is shown that the exact capacity of pools qualified to participate in the market can be found using a reliability assessment overall components that

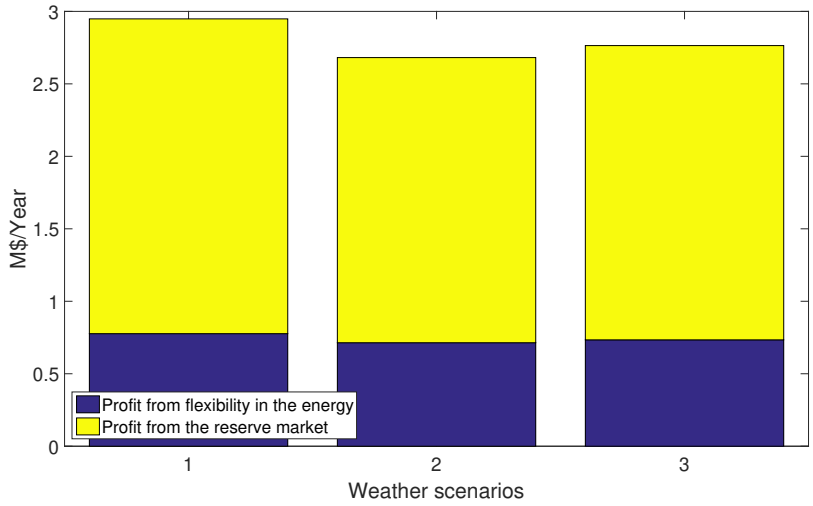

Figure 3.21: Profit comparision for different weather scenarios.

can interrupt the connectivity of the control center and a pool pump. Based on the capacity credit from the pools, an optimal bidding strategy is formulated for the aggregators to participate in the day-ahead reserve markets. By utilizing a scenario-based approach, it is shown that it can save up to 27% in the realization cost of procurement strategy. A cost-benefit analysis is performed to demonstrate the investment strategy for the aggregators using the ERCOT market as an example.

Common mode failures, and disabling the control option is also added to the reliability framework model on top of modeling ISP failure possibility. It was shown that the PDF of aggregated pool availability changes when we consider all these factors, however, the changes are not impacting the results to enter the operational planning stage significantly.

This section opens several avenues for future work. On the reliability assessment side, currently we regard two devices, with and WiFi network independent, but some common mode failures can impact both at the same time as discussed in [97]. Also, we have not yet modeled other components in the communication network such as Internet Service Providers (ISOs) in our reliability package. Last but not least, since the methods of capacity credit assessments are different from what shown here, a comparison between the amount that is qualified for the market (current approach) and amount of capacity credit will be among our future works.

On the operational planning side, a few topics need further research. First, a process to generate IID samples from raw price data needs to be added to rigorously guarantee the risk same as Chapter 2. This topic is under further research and an early publication is available in [50]. Robust formulations cannot be suitable for the purpose of price forecast scenarios since the uncertainty set of robust methods in ERCOT can vary from $[-250, 9000]$ and might come with an ineffective solution. Simplifying the uncertainty set as in [98] is one approach to avoid conservative solutions. However, first, it guarantees the optimality only if realizations of uncertainty occur inside the predefined uncertainty set or dynamically evolving uncertainty set, and second, the level of conservativeness is defined by the length of the uncertainty set. As mentioned for prices of energy, this length can vary from a negative price (for energy price) to the price cap, based on the Lagrangian multipliers in the economic dispatch problem ISO solves [99]. Second, the number of hours pools should remain {ON} before turning {OFF} in this proposal is set to be one hour due to price forecast resolution. However, the number of {ON,OFF} operation per day can have an impact on the customer's cost as well as cleaning performance which needs further research.

Last but not least, a reinforcement learning strategy can replace the reliability assessment package by learning from an individual customer's past response to potentially use more capacity in the market.

4. SUMMARY AND CONCLUSIONS

This dissertation introduces two practical approaches to gain flexibility in the power systems operations along with one compelling data-driven optimization technique to account for the growing uncertainty. Along with the introduction of the data-driven method named as *scenario approach*, we exploited the structure of power system economic dispatch and revealed its unique characteristics making the scenario theory a powerful and rigorous method for solving it.

It was shown that while there have been some past works on using the scenario theory in power systems scheduling, we are the first to address its adaptability for the structure of power system problems. This structure helps the scenario theory to uses much less number of scenarios and therefore making it scalable to the real power system operations.

For this purpose, we divided the economic dispatch problem into two parts. The part that congestion is not expected and the part that congestion consideration into the economic dispatch would be essential. For the former, we showed how we can know exactly how many of scenarios would be of a support scenario and therefore we can use that number as the complexity of the problem in the scenario theory making the number of scenarios not growing with the size of the system. For the times that the solution is not desired or conservative samples are expected, we introduced a scenario reduction technique that we can remove scenarios of choice with a controlled risk increment. In this approach, we essentially trading risk for performance and filtering out possible *bad* samples. The stage where we solve the problem while knowing the risk parameters of the scenario approach in-advance is being called *a-priori* solution in this dissertation. This will be in contrast with the results for a system while we consider congestion.

When network parameters are important, for instance in peak hours or when lines are near their fully loaded thresholds, we introduced a *a-posteriori* solution. Basically, in such a condition we solve the system using a number of samples and observe the solution. The complexity of the solution will give us the a-posteriori level of risk parameter. We showed that this new risk parameter for the case of power system operations can be much lower and we can move from a

sample set with essentially no risk guarantee in the a-priori, to a very tight risk guarantee in the a posteriori. This is a key result, making the scenario method scalable in a general case to the power system operations.

The above-mentioned development of scenario theory requires convexity of the problem and therefore we used it in the real-time economic dispatch and day ahead optimal bidding strategy of aggregation of small load and their participation in the wholesale spinning reserve market. More precisely we focused on the in-house swimming pool pumps capacity aggregation and participation in the market. Since residential loads cannot be compared with conventional power plants with a firm capacity, we developed a reliability assessment framework to come up with the capacity that can be participated in the wholesale market. Then with a given capacity for each hour and the forecasts on the prices we formulated and solved an operational planning stage to decide the strategy utility should take for each hour of the next day. We also used the scenario theory as price scenarios instead of a forecast and showed it will be of a benefit to do so and hedge against potential price uncertainties. Finally, we concluded with a cost-benefit analysis showing the promising future of such an approach. A summary of all proposed and studies approaches in this dissertation is shown in Fig. 4.1.

4.1 Challenges

One potential challenge to the scenario theory application in power system is how to generate appropriate samples from the raw data. Basically, scenario theory required the samples to be independent and identically distributed. Raw data might not have this property and when you gather more and more of the raw data, this quality will be more endangered because the underlying distribution of uncertainty might be dynamically changing. However, based on our knowledge there are already efforts on generating unlimited samples from raw data and more results are expected to be revealed in the near future.

The biggest challenge ahead of aggregation of small loads and their participation in the wholesale market is the legal barriers. While there is no law against the aggregation, there are not enough rulings in place to allow such aggregation. Also, typical reserve providers in the system should be

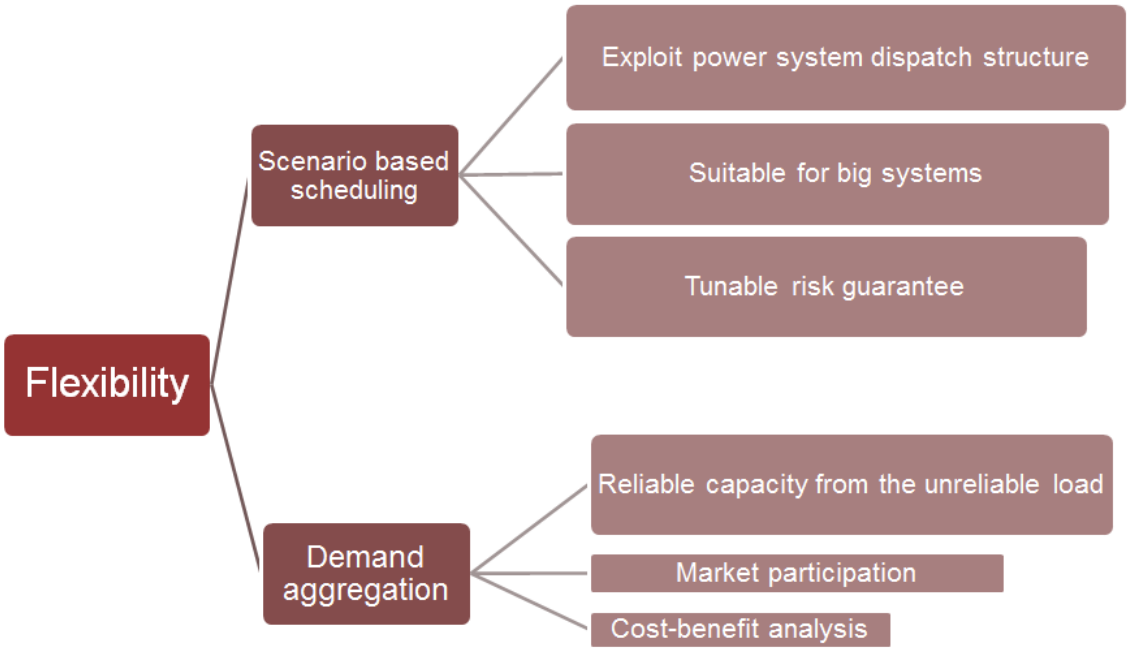

Figure 4.1: A graphical illustration of the proposed approached in the dissertation.

equipped with an under frequency relay and trip in a very fast fashion, Such relays are expensive and installing them in each house would be impossible. Therefore a replacement for such operations needs to be in place or current protocols should address this type of aggregation separately.

4.2 Further Study

The next step in the scenario theory application to power system problems is using it to solve the Unit Commitment problem. Clearly, the original theory requires convexity and is not suitable for such an application. However, recently new advances [100] on the theory showed a promising direction for the case of unit commitment which we are in the process of testing it. The next step for the aggregation of unreliable loads is replacing the reliability assessment with a reinforcement learning approach to first be able to model and update each customer's performance separately. Second, it allows us to start with a very small pool of customers and gain reliable capacity from them and progressively move towards a larger number of customers. Third, while multiple reserve deployments of swimming pools or flexible demands under current approach might cause over or

under deployments, our initial tests showed that reinforcement learning approach would not have such a drawback and gives promising results.

While the above details were technical improvements, a utility deployment of such an approach can be the ultimate future work for the swimming pools work. As shown it can change the way we think about demand response to a response with financial *and* comfort gains. The author believes the combination of the two is essential for a demand response strategy to be successful and sustainable.

REFERENCES

[1] "ERCOT quick facts." Available at http://www.ercot.com/content/wcm/lists/114739/ERCOT_Quick_Facts_4317.pdf, (Date last accessed 24-October-2017).

[2] L. Soder, "Reserve margin planning in a wind-hydro-thermal power system," *IEEE Transactions on Power Systems*, vol. 8, pp. 564–571, May 1993.

[3] L. Xie, P. M. S. Carvalho, L. A. F. M. Ferreira, J. Liu, B. H. Krogh, N. Popli, and M. D. Ilic, "Wind integration in power systems: Operational challenges and possible solutions," *Proceedings of the IEEE*, vol. 99, pp. 214–232, Jan 2011.

[4] M. Hedayati-Mehdiabadi, K. W. Hedman, and J. Zhang, "Reserve policy optimization for scheduling wind energy and reserve," *IEEE Transactions on Power Systems*, vol. PP, no. 99, pp. 1–1, 2017.

[5] J. B. Cardell and C. L. Anderson, "A flexible dispatch margin for wind integration," *IEEE Transactions on Power Systems*, vol. 30, no. 3, pp. 1501–1510, 2015.

[6] P. Xiong and C. Singh, "Optimal planning of storage in power systems integrated with wind power generation," *IEEE Transactions on Sustainable Energy*, vol. 7, no. 1, pp. 232–240, 2016.

[7] Y. Xu and C. Singh, "Power system reliability impact of energy storage integration with intelligent operation strategy," *IEEE Transactions on smart grid*, vol. 5, no. 2, pp. 1129–1137, 2014.

[8] M. S. Modarresi, L. Xie, M. Campi, S. Garatti, A. Carè, A. Thatte, and P. R. Kumar, "Scenario-based economic dispatch with tunable risk levels in high-renewable power systems," *IEEE Transactions on Power Systems*, pp. 1–1, 2018.

[9] M. S. Modarresi, L. Xie, , and C. Singh, "Reserves from controllable swimming pool pumps: Reliability assessment and operational planning," in *2018 51st Hawaii International Con-*

ference on System Sciences (HICSS), Jan 2018.

[10] "ERCOT quick facts." (Date last accessed 30-September-2018).

[11] "2016 LTSA update." (Date last accessed 30-September-2018).

[12] P. P. Varaiya, F. F. Wu, and J. W. Bialek, "Smart Operation of Smart Grid: Risk-Limiting Dispatch," *Proceedings of the IEEE*, vol. 99, no. 1, pp. 40–57, 2011.

[13] R. Entriken, P. Varaiya, F. Wu, J. Bialek, C. Dent, A. Tuohy, and R. Rajagopal, "Risk limiting dispatch," in *2012 IEEE Power and Energy Society General Meeting*, pp. 1–5, July 2012.

[14] L. Wu, M. Shahidehpour, and T. Li, "Stochastic Security-Constrained Unit Commitment," *IEEE Transactions on Power Systems*, vol. 22, no. 2, pp. 800–811, 2007.

[15] A. Papavasiliou, S. S. Oren, and R. P. O. Neill, "Reserve Requirements for Wind Power Integration: A Stochastic Programming Framework," *IEEE Transactions on Power Systems*, vol. 26, no. 4, pp. 2197–2206, 2011.

[16] D. Bertsimas, E. Litvinov, X. A. Sun, J. Zhao, and T. Zheng, "Adaptive Robust Optimization for the Security Constrained Unit Commitment Problem," *IEEE Transactions on Power Systems*, vol. 28, no. 1, pp. 52–63, 2013.

[17] N. Zhang, C. Kang, Q. Xia, Y. Ding, Y. Huang, R. Sun, J. Huang, and J. Bai, "A convex model of risk-based unit commitment for day-ahead market clearing considering wind power uncertainty," *IEEE Transactions on Power Systems*, vol. 30, pp. 1582–1592, May 2015.

[18] D. Ross and S. Kim, "Dynamic Economic Dispatch of Generation," *IEEE Transactions on Power Apparatus and Systems*, vol. PAS-99, no. 6, pp. 2060–2068, 1980.

[19] Y. Gu and L. Xie, "Early detection and optimal corrective measures of power system insecurity in enhanced look-ahead dispatch," *IEEE Transactions on Power Systems*, vol. 28, no. 2, pp. 1297–1307, 2013.

[20] Z. Li, W. Wu, B. Zhang, and H. Sun, "Efficient Location of Unsatisfiable Transmission Constraints in Look-Ahead Dispatch via an Enhanced Lagrangian Relaxation Framework," vol. 30, no. 3, pp. 1–10, 2014.

[21] Á. Lorca and X. A. Sun, "Adaptive Robust Optimization With Dynamic Uncertainty Sets for Multi-Period Economic Dispatch," *IEEE Transactions on Power Systems*, vol. 30, no. 4, pp. 1702–1713, 2015.

[22] Q. Wang and B. M. Hodge, "Enhancing power system operational flexibility with flexible ramping products: A review," *IEEE Transactions on Industrial Informatics*, vol. 13, pp. 1652–1664, Aug 2017.

[23] H. Nosair and F. Bouffard, "Economic dispatch under uncertainty: The probabilistic envelopes approach," *IEEE Transactions on Power Systems*, vol. 32, pp. 1701–1710, May 2017.

[24] C. Tang, J. Xu, Y. Sun, J. Liu, X. LI, D. Ke, J. Yang, and X. Peng, "Look-ahead economic dispatch with adjustable confidence interval based on a truncated versatile distribution model for wind power," *IEEE Transactions on Power Systems*, vol. PP, no. 99, pp. 1–1, 2017.

[25] Y. Gu and L. Xie, "Stochastic Look-Ahead Economic Dispatch With Variable Generation Resources," *IEEE Transactions on Power Systems*, pp. 1–13, 2016.

[26] A. A. Thatte and L. Xie, "A metric and market construct of inter-temporal flexibility in time-coupled economic dispatch," *IEEE Transactions on Power Systems*, vol. 31, no. 5, pp. 3437–3446, 2016.

[27] A. A. Thatte, X. A. Sun, and L. Xie, "Robust optimization based economic dispatch for managing system ramp requirement," *Proceedings of the Annual Hawaii International Conference on System Sciences*, pp. 2344–2352, 2014.

[28] A. Ben-Tal and A. Nemirovski, "Robust convex optimization," *Mathematics of operations research*, vol. 23, no. 4, pp. 769–805, 1998.

[29] L. El Ghaoui, F. Oustry, and H. Lebret, "Robust solutions to uncertain semidefinite programs," *SIAM Journal on Optimization*, vol. 9, no. 1, pp. 33–52, 1998.

[30] A. Ben-Tal and A. Nemirovski, "On tractable approximations of uncertain linear matrix inequalities affected by interval uncertainty," *SIAM Journal on Optimization*, vol. 12, no. 3, pp. 811–833, 2002.

[31] G. Calafiore and M. C. Campi, "The scenario approach to robust control design," *IEEE Transactions on Automatic Control*, vol. 51, no. 5, pp. 742–753, 2006.

[32] A. Prékopa, *Stochastic programming*. Springer Science & Business Media, 2013.

[33] M. W. Tanner and L. Ntaimo, "IIS branch-and-cut for joint chance-constrained stochastic programs and application to optimal vaccine allocation," *European Journal of Operational Research*, vol. 207, no. 1, pp. 290 – 296, 2010.

[34] B. Zeng, Y. An, and L. Kuznia, "Chance constrained mixed integer program: Bilinear and linear formulations, and benders decomposition," *Mathematical Programming (to appear)*, 2017.

[35] A. Nemirovski and A. Shapiro, "Convex approximations of chance constrained programs," *SIAM Journal on Optimization*, vol. 17, no. 4, pp. 969–996, 2006.

[36] A. Ben-Tal, L. El Ghaoui, and A. Nemirovski, *Robust optimization*. Princeton University Press, 2009.

[37] M. C. Campi and S. Garatti, "The Exact Feasibility of Randomized Solutions of Uncertain Convex Programs," *SIAM Journal on Optimization*, vol. 19, no. 3, pp. 1211–1230, 2008.

[38] M. C. Campi and S. Garatti, "A sampling-and-discarding approach to chance-constrained optimization: feasibility and optimality," *Journal of Optimization Theory and Applications*, vol. 148, no. 2, pp. 257–280, 2011.

[39] K. Margellos, P. Goulart, and J. Lygeros, "On the road between robust optimization and the scenario approach for chance constrained optimization problems," *IEEE Transactions on Automatic Control*, vol. 59, pp. 2258–2263, Aug 2014.

[40] S. Grammatico, X. Zhang, K. Margellos, P. Goulart, and J. Lygeros, "A scenario approach to non-convex control design: Preliminary probabilistic guarantees," in *2014 American Control Conference*, pp. 3431–3436, June 2014.

[41] M. Vrakopoulou, K. Margellos, J. Lygeros, and G. Andersson, "A probabilistic framework for reserve scheduling and N-1 security assessment of systems with high wind power penetration," *IEEE Transactions on Power Systems*, vol. 28, no. 4, pp. 3885–3896, 2013.

[42] Y. Zhang, S. Shen, and J. L. Mathieu, "Distributionally robust chance-constrained optimal power flow with uncertain renewables and uncertain reserves provided by loads," *IEEE Transactions on Power Systems*, vol. 32, pp. 1378–1388, March 2017.

[43] M. Vrakopoulou, B. Li, and J. L. Mathieu, "Chance constrained reserve scheduling using uncertain controllable loads part I: Formulation and scenario-based analysis," *IEEE Transactions on Smart Grid*, 2017.

[44] H. Ming, L. Xie, M. C. Campi, S. Garatti, and P. R. Kumar, "Scenario-based economic dispatch with uncertain demand response," *IEEE Transactions on Smart Grid (accepted, to appear)*, 2017.

[45] M. Amini and M. Almassalkhi, "Trading off robustness and performance in receding horizon control with uncertain energy resources," in *2018 Power Systems Computation Conference (PSCC)*, pp. 1–7, IEEE, 2018.

[46] M. C. Campi and S. Garatti, "Wait-and-judge scenario optimization," *Mathematical Programming*, vol. 167, no. 1, pp. 155–189, 2018.

[47] A. J. Wood and B. F. Wollenberg, *Power generation, operation, and control*. John Wiley & Sons, 2012.

[48] G. Calafiore and M. C. Campi, "Uncertain convex programs: randomized solutions and confidence levels," *Mathematical Programming*, vol. 102, no. 1, pp. 25–46, 2005.

[49] A. A. Thatte, Y. Li, and L. Xie, "Managing system ramp flexibility by utilizing price-responsive demand: An empirical assessment," in *2016 49th Hawaii International Conference on System Sciences (HICSS)*, pp. 2345–2353, IEEE, 2016.

[50] H. A. Nasir, T. Zhao, A. Carè, Q. J. Wang, and E. Weyer, "Efficient river management using stochastic MPC and ensemble forecast of uncertain in-flows," in *IFAC-PapersOnLine*, pp. 37–42, Elsevier, 2018.

[51] S. Garatti and M. C. Campi, "Modulating robustness in control design: Principles and algorithms," *IEEE Control Systems*, vol. 33, pp. 36–51, April 2013.

[52] T. Zheng and E. Litvinov, "On ex post pricing in the real-time electricity market," *IEEE Transactions on Power Systems*, vol. 26, no. 1, pp. 153–164, 2011.

[53] T. Zheng and E. Litvinov, "Ex post pricing in the co-optimized energy and reserve market," *IEEE Transactions on Power Systems*, vol. 21, no. 4, pp. 1528–1538, 2006.

[54] A. L. Ott, "Experience with PJM market operation, system design, and implementation," *IEEE Transactions on Power Systems*, vol. 18, no. 2, pp. 528–534, 2003.

[55] F. Li, Y. Wei, and S. Adhikari, "Improving an unjustified common practice in ex post LMP calculation," *IEEE Transactions on Power Systems*, vol. 25, no. 2, pp. 1195–1197, 2010.

[56] D. H. Choi and L. Xie, "Economic impact assessment of topology data attacks with virtual bids," *IEEE Transactions on Smart Grid*, vol. 9, pp. 512–520, March 2018.

[57] W. W. Hogan *et al.*, "Financial transmission rights, revenue adequacy and multi-settlement electricity markets," *unpublished.[Online]. Available Harvard University web site: http://www. hks. harvard. edu/fs/whogan/Hogan_FTR_Rev_Adequacy_*, vol. 31813, 2012.

[58] M. C. Campi, S. Garatti, and M. Prandini, "The scenario approach for systems and control design," *IFAC Proceedings Volumes*, vol. 41, no. 2, pp. 381–389, 2008.

[59] G. Schildbach, L. Fagiano, and M. Morari, "Randomized solutions to convex programs with multiple chance constraints," *SIAM Journal on Optimization*, vol. 23, no. 4, pp. 2479–2501, 2013.

[60] X. Zhang, S. Grammatico, G. Schildbach, P. Goulart, and J. Lygeros, "On the sample size of random convex programs with structured dependence on the uncertainty," *Automatica*, vol. 60, pp. 182–188, 2015.

[61] A. Carè, S. Garatti, and M. C. Campi, "Fast-fast algorithm for the scenario technique," *Operations Research*, vol. 62, no. 3, pp. 662–671, 2014.

[62] M. C. Campi and A. Carè, "Random convex programs with L_1-regularization: Sparsity and generalization," *SIAM Journal on Control and Optimization*, vol. 51, no. 5, pp. 3532–3557, 2013.

[63] V. L. Levin, "Application of E. Helly's theorem to convex programming, problems of best approximation and related questions," *Sbornik: Mathematics*, vol. 8, no. 2, pp. 235–247, 1969.

[64] A. B. Birchfield, K. M. Gegner, T. Xu, K. S. Shetye, and T. J. Overbye, "Statistical considerations in the creation of realistic synthetic power grids for geomagnetic disturbance studies," *IEEE Transactions on Power Systems*, vol. 32, pp. 1502–1510, March 2017.

[65] R. D. Zimmerman, C. E. Murillo-Sanchez, and R. J. Thomas, "MATPOWER: Steady-state operations, planning, and analysis tools for power systems research and education," *IEEE Transactions on Power Systems*, vol. 26, pp. 12–19, Feb 2011.

[66] D. Angeli and P.-A. Kountouriotis, "A stochastic approach to "dynamic-demand" refrigerator control," *IEEE Transactions on control systems technology*, vol. 20, no. 3, pp. 581–592, 2012.

[67] E. Vrettos, F. Oldewurtel, and G. Andersson, "Robust energy-constrained frequency reserves from aggregations of commercial buildings," *IEEE Transactions on Power Systems*, vol. 31, no. 6, pp. 4272–4285, 2016.

[68] J. MacDonald, P. Cappers, D. Callaway, and S. Kiliccote, "Demand response providing ancillary services," *Grid-Interop*, 2012.

[69] M. Amini and M. Almassalkhi, "Investigating delays in frequency-dependent load control," in *2016 IEEE Innovative Smart Grid Technologies-Asia (ISGT-Asia)*, pp. 448–453, IEEE, 2016.

[70] J. H. Eto, J. Nelson-Hoffman, C. Torres, S. Hirth, B. Yinger, J. Kueck, B. Kirby, C. Bernier, R. Wright, A. Barat, *et al.*, "Demand response spinning reserve demonstration," *Lawrence Berkeley National Laboratory*, 2007.

[71] "Current protocols - nodal." Available at http://www.ercot.com/mktrules/nprotocols/current, (Date last accessed 24-October-2017).

[72] W. Jewell, "Residential energy efficiency and electric demand response," in *2016 49th Hawaii International Conference on System Sciences (HICSS)*, pp. 2435–2444, Jan 2016.

[73] S. Meyn, P. Barooah, A. Bušić, and J. Ehren, "Ancillary service to the grid from deferrable loads: The case for intelligent pool pumps in florida," in *52nd IEEE Conference on Decision and Control*, pp. 6946–6953, Dec 2013.

[74] P. Barooah, A. Buic, and S. Meyn, "Spectral decomposition of demand-side flexibility for reliable ancillary services in a smart grid," in *2015 48th Hawaii International Conference on System Sciences (HICSS)*, pp. 2700–2709, Jan 2015.

[75] S. P. Meyn, P. Barooah, A. Bušić, Y. Chen, and J. Ehren, "Ancillary service to the grid using intelligent deferrable loads," *IEEE Transactions on Automatic Control*, vol. 60, no. 11, pp. 2847–2862, 2015.

[76] "Programming suggestions for centrifugal pumps." Available at http://www.wentec.com/unipower/miscellaneous/pdf/centrifugalpump.pdf, (Date last accessed 24-October-2017).

[77] "Intelliflo Vf pump installation and user's guide." Available at http://www.pentairpool.com, (Date last accessed 24-October-2017).

[78] "Nodal 101." Available at http://www.ercot.com/services/training/course/109518# materials, (Date last accessed 24-October-2017).

[79] "Residential pools." Available at http://www.houstontx.gov/health/Environmental/residentialpools.html, (Date last accessed 24-October-2017).

[80] "What causes algae problems?." Available at http://www.poolcenter.com/algae, (Date last accessed 24-October-2017).

[81] "Wemo mini smart plug." Available at http://www.belkin.com/us/F7C063-Belkin/p/P-F7C063/, (Date last accessed 24-October-2017).

[82] "Sonoff - wifi wireless smart switch." Available at https://www.itead.cc/smart-home/sonoff-wifi-wireless-switch.html, (Date last accessed 24-October-2017).

[83] "Smart wifi meter plug 31." Available at http://www.orvibo.com/en/product/47.html, (Date last accessed 24-October-2017).

[84] "smart wifi switch." Available at https://goo.gl/J0T2WU, (Date last accessed 24-October-2017).

[85] "Amazon alexa." Available at https://developer.amazon.com/alexa, (Date last accessed 24-October-2017).

[86] F. Kamyab, M. Amini, S. Sheykhha, M. Hasanpour, and M. M. Jalali, "Demand response program in smart grid using supply function bidding mechanism," *IEEE Transactions on Smart Grid*, vol. 7, pp. 1277–1284, May 2016.

[87] R. Billinton and R. N. Allan, *Reliability evaluation of engineering systems*. Plenum Press, 1992.

[88] C. Singh and R. Billinton, *System reliability, modelling and evaluation*, vol. 769. Hutchinson London, 1977.

[89] M. Bebbington, C.-D. Lai, and R. Zitikis, "Useful periods for lifetime distributions with bathtub shaped hazard rate functions," *IEEE Transactions on Reliability*, vol. 55, no. 2, pp. 245–251, 2006.

[90] H. Pham and C.-D. Lai, "On recent generalizations of the weibull distribution," *IEEE transactions on reliability*, vol. 56, no. 3, pp. 454–458, 2007.

[91] A. Halder, X. Geng, P. R. Kumar, and L. Xie, "Architecture and algorithms for privacy preserving thermal inertial load management by a load serving entity," *IEEE Transactions on Power Systems*, vol. PP, no. 99, pp. 1–1, 2017.

[92] A. Carè, S. Garatti, and M. C. Campi, "Scenario min-max optimization and the risk of empirical costs," *SIAM Journal on Optimization*, vol. 25, no. 4, pp. 2061–2080, 2015.

[93] Y. Pan, "Top 10 cities for making a splash in an amazing home swimming pool." Available at http://www.realtor.com/news/trends/top-10-cities-for-pool-loving-homeowners/, (Date last accessed 24-October-2017).

[94] "Google earth view of plano residential area." Available at https://goo.gl/eU8zOP, (Date last accessed 24-October-2017).

[95] "United states census bureau." Available at https://www.census.gov/, (Date last accessed 24-October-2017).

[96] "Day-ahead market." Available at http://www.ercot.com/mktinfo/dam, (Date last accessed 24-October-2017).

[97] M. Papic and *et. al*, "Research on common-mode and dependent (cmd) outage events in power systems: A review," *IEEE Transactions on Power Systems*, vol. 32, pp. 1528–1536, March 2017.

[98] A. A. Thatte and L. Xie, "A robust model predictive control approach to coordinating wind and storage for joint energy balancing and frequency regulation services," in *2015 IEEE Power Energy Society General Meeting*, pp. 1–5, July 2015.

[99] A. A. Thatte, X. A. Sun, and L. Xie, "Robust optimization based economic dispatch for managing system ramp requirement," in *2014 47th Hawaii International Conference on System Sciences (HICSS)*, pp. 2344–2352, Jan 2014.

[100] M. C. Campi, S. Garatti, and F. A. Ramponi, "A general scenario theory for non-convex optimization and decision making," *IEEE Transactions on Automatic Control*, 2018.

APPENDIX

SC-LAED LOCATIONAL MARGINAL PRICING[1]

Table A.1: Appendix Nomenclature

Sets:	
$\mathbf{CL}^+/\mathbf{CL}^-$	Set of positively/negatively congested lines.
Parameters and constants:	
$\hat{P}_{g_i}$	Decision input from binding interval of Sc-LAED.
ρ	Energy balance equation shadow price.
ϱ_{max}	Shadow price corresponded to a positively congested lines.
ϱ_{min}	Shadow price corresponded to a negatively congested lines.
ς	Shadow price for generation capacity constraint.
Decision variables:	
P_{g_i}	Power generation for g_i.

[1]This section is in part a reprint of the material in the following papers: Reprinted with permission from M. Sadegh Modarresi, Le Xie, *et al.*, "Scenario-based Economic Dispatch with Tunable Risk Levels in High-renewable Power Systems," in IEEE Transactions on Power Systems. DOI: 10.1109/TPWRS.2018.2874464, Copyright 2018, IEEE.

$$\min_{P_{g_i}[t]} \quad z = \sum_{i=1}^{N_g} c_{g_i} P_{g_i} \tag{A.1a}$$

s.t.

$$\rho \quad \sum_{i=1}^{N_g} P_{g_i} = \sum_{i=1}^{N_g} \hat{P}_{g_i} \tag{A.1b}$$

$$\varrho_{max} \quad \sum_{j=1}^{N_b} PTDF_{\mathbf{e}}^{\varpi^+} \mathcal{P}_{\mathbf{n}}^{\varpi^+} \leq \overline{F^{\varpi^+}}, \quad \forall \varpi^+ \in \mathbf{CL}^+, \tag{A.1c}$$

$$\varrho_{min} \quad \sum_{j=1}^{N_b} PTDF_{\mathbf{e}}^{\varpi^-} \mathcal{P}_{\mathbf{n}}^{\varpi^-} \geq -\overline{F^{\varpi^-}}, \quad \forall \varpi^- \in \mathbf{CL}^-, \tag{A.1d}$$

$$\varsigma \quad \hat{P}_{g_i}^{min} \leq P_{g_i} \leq \hat{P}_{g_i}^{max} \quad \forall i = 1, 2, \ldots, N_g. \tag{A.1e}$$

The presented LMP calculation process is based on equations (1) to (5) in [55]. For simplicity, here we have assumed loss-less system. In the following optimization problem, a *hat* symbol represents the input to the problem from the Sc-LAED. The objective is to minimize total generation cost (A.1a). $(A.1b)$ is energy balancing constraint to satisfy the same demand as (2.5b). For a set of positively and negatively congested lines in (A.1c) and (A.1d) return shadow prices corresponding to the line constraints. Capacity constraint of each generator embedded with its incremental ramping up $\Delta P_{g_i}^{max}$ and down $\Delta P_{g_i}^{min}$ limit of such generator is shown in (A.1e), where $\hat{P}_{g_i}^{max} = \hat{P}_{g_i} + \Delta P_{g_i}^{max}$ and $\hat{P}_{g_i}^{min} = \hat{P}_{g_i} + \Delta P_{g_i}^{min}$.

The $N_b \times 1$ vector of nodal LMP can be reached by (A.2). $\mathbf{1}_{N_b}$ is a $N_b \times 1$ all ones column vector, and ϱ_{κ}^{max} and ϱ_{κ}^{min} are $N_l \times 1$ column matrices containing ϱ^{max} and ϱ^{min} on the rows corresponding to a positively or negatively congested line respectively.

$$\mathbf{LMP} = \rho(\kappa) \times \mathbf{1}_{N_b} - PTDF_{\mathbf{e}}' \times (\varrho_{\kappa}^{max} - \varrho_{\kappa}^{min}) \tag{A.2}$$